Noname manuscript No.
(will be inserted by the editor)

Magnetic Fields in Astrophysical Jets: From Launch to Termination

Ralph E. Pudritz · Martin J. Hardcastle · Denise C. Gabuzda

arXiv:1205.2073v1 [astro-ph.HE] 9 May 2012

Received: date / Accepted: date

Abstract Long-lived, stable jets are observed in a wide variety of systems, from protostars, through Galactic compact objects to active galactic nuclei (AGN). Magnetic fields play a central role in launching, accelerating, and collimating the jets through various media. The termination of jets in molecular clouds or the interstellar medium deposits enormous amounts of mechanical energy and momentum, and their interactions with the external medium, as well, in many cases, as the radiation processes by which they are observed, are intimately connected with the magnetic fields they carry. This review focuses on the properties and structures of magnetic fields in long-lived jets, from their launch from rotating magnetized young stars, black holes, and their accretion discs, to termination and beyond. We compare the results of theory, numerical simulations, and observations of these diverse systems and address similarities and differences between relativistic and non-relativistic jets in protostellar versus AGN systems. On the observational side, we focus primarily on jets driven by AGN because of the strong observational constraints on their magnetic field properties, and we discuss the links between the physics of these jets on all scales.

Keywords magnetic fields · jets · polarization · radio continuum: galaxies · X-rays: galaxies

1 Introduction

Astrophysical jets have been discovered in a very wide range of physical systems, from regions of star formation, to gamma-ray bursters and stellar black holes, on up in scale and

Ralph Pudritz
Dept. of Physics and Astronomy, McMaster University, Hamilton, ON L8S 4M1, Canada
E-mail: pudritz@mcmaster.ca

Martin Hardcastle
School of Physics, Astronomy & Mathematics, University of Hertfordshire, College Lane, Hatfield AL10 9AB, UK
E-mail: m.j.hardcastle@herts.ac.uk

Denise Gabuzda
Physics Department, University College Cork, Republic of Ireland
E-mail: d.gabuzda@ucc.ie

energy to the nuclei of giant radio galaxies and quasars. They are often associated with accretion discs and their launch, internal dynamics, and impact upon their surroundings are of ongoing importance and significance over a whole range of astrophysical phenomena — from the parsec (pc) scales that characterize the impact of jets from young stellar objects within their natal molecular clouds, to the megaparsec (Mpc) scales of giant clusters of galaxies whose intercluster media are significantly stirred and heated by jets emanating from the cores of active galaxies (e.g., Dunn and Fabian 2006). On stellar scales, jets from young stellar objects (YSOs) span the breadth of the stellar mass spectrum: from massive stars such as W33A which shows a hot fast jet when observed in Br γ lines as well as an underlying accretion disc (Davies et al. 2010), to the well known solar-mass systems such as classical T-Tauri stars (TTS) (see Ray et al. 2007, for a review), and on down into the brown dwarfs (e.g., Whelan et al. 2009). There is good evidence that all of the protostellar systems are associated with discs. Stellar mass black holes, otherwise known as microquasars (Mirabel 2005) are also very active sources of relativistic jets. On extragalactic scales, jets are observed to be associated with accretion on to supermassive black holes (up to a few billion solar masses) in the centres of active galaxies (Blandford 2001). Models for gamma-ray bursts (GRBs), which are also located at cosmological distances, focus on either the collapse of massive stars or the merger of two compact stellar objects to form a black hole in a process that releases about a solar mass worth of gravitational potential energy and which generates a highly relativistic magnetized jet (Mészáros 2012).

Given the vast range in energies, scales, and details spanned by these diverse systems, it is intriguing that accreting systems seen in nature make such extensive and ubiquitous use of energetic outflows as part of their evolution. Is there a universal mechanism at work that almost guarantees that jets will be present? What is the basic physical mechanism that creates and drives jets across all of these scales? What role do they play in the evolution of such accreting compact systems? The fact that all these systems share common physical components — central gravitating sources, accretion discs, and magnetic fields — provides the unifying foundation on which theoretical models are constructed and observationally tested.

Magnetic fields play a critical role in creating, driving, and directing the evolution of jets. Indeed, the successful existing models of jets in these diverse systems invoke magnetic fields threading central objects such as gaseous accretion discs or rapidly rotating central objects themselves (see reviews by, e.g., Shu et al. 2000; Pudritz et al. 2007). The release of gravitational potential energy during accretion is a key power source for most of these jets. The great utility of magnetic torques is that they can readily tap into the shear energy available in the accretion discs that form as a consequence of gravitational collapse. Models of magnetized outflows from accretion discs in AGN, developed by Blandford and Payne (1982), were applied soon after to understanding jets in protostellar systems (Pudritz and Norman 1983, 1986). These theories envisage that material from a disc, in being forced to co-rotate with a threading magnetic field, is flung outwards along sufficiently inclined, open field lines. The gas continues to accelerate as long as the field is strong enough to maintain co-rotation with the central disc, or rotor. The inertia of this matter moving along the field line causes the field to wrap up in a toroidal-like structure — creating a helical field. It is this dominant, outer toroidal field component that exerts a pinching force upon the jet, collimating it towards the axis. A second major prediction of this basic theory is that jets should be extracting the angular momentum of their sources, and jet rotation is a key prediction of the models. Another abundant source of energy resides in the rotation available in rapidly rotating black holes or pulsars, and once again it is known that electromagnetic torques can tap rotational energy efficiently (Blandford and Znajek 1977). So for rapidly ac-

creting or spinning objects, large scale magnetic fields appear to be nature's preferred tool in extracting energy and angular momentum and directing them in the formation of ordered, magnetically collimated, outflows.

Observations of crucial properties of jets, such as their densities, temperatures, velocity structure, and magnetic fields, vary quite considerably between protostellar and extragalactic systems. In the former, forbidden line emission (FLER) produced by shocks in the jet allows one to measure directly everything with the exception of the magnetic field. On the other hand, extragalactic jets emit synchrotron radiation which arises from the relativistic electrons that spiral around magnetic field lines. This radiation allows one directly to measure the direction of the magnetic field in the jet, and to estimate its strength. However, the absence of distinct emission lines from the outflowing material itself in AGN jets prevents one from measuring the other crucial physical variables. It is for this reason that protostellar systems have become such important laboratories for jet studies. Until 2010, these limitations prevented direct observational comparison of these classes of jets, and, as a result, meant that it was impossible to test whether or not jets have a universal magnetic field based mechanism. This all changed with the discovery of synchrotron radiation from the protostellar jet, HH 80-81 (Carrasco-González et al. 2010). Relativistic electrons in otherwise non-relativistic jets arise from acceleration in the jet's terminal shock. The results show that the magnetic structures of protostellar and AGN jets are similar — with a field parallel to the jet axis at the centre and a surrounding helical field towards the jet edges.

In this paper, we examine the structure and role of magnetic fields in the physics of jets — from their launch on discs or compact rotors, to their dynamics and evolution, and finally to a consideration of how such strongly magnetized flows affect their environments on these various scales. We begin our analysis with non-relativistic systems — the protostellar jets that are a ubiquitous and vital component of any star-forming region (Section 2). We also summarize the theory and simulations of relativistic jets in the context of AGNs. (We do not consider the impulsive, short-lived jets in gamma-ray bursts, although much of the same physics is expected to apply, as the observational challenges are very different; the reader is referred to reviews by Piran (2004) and Granot (2007).) In Section 3 we then turn to relativistic systems and discuss the measurement of the structure and dynamics of AGN jets on highly compact (pc) scales, probing the conditions near at the source of the jets using VLBI. The magnetic structure of jets on these scales is probably a reflection of their internal dynamics and not of the shocks which occur throughout the body of the jets. Indeed, the mounting evidence for helical magnetic fields in extragalactic jets, taken with the newly discovered evidence for helical fields in protostellar jets discussed above, strongly suggest that the physical mechanism of collimation may be the same. Finally, we go out to the scales of jet termination (Section 4), focussing on the evidence for magnetic field properties on these largest scales and exploring the connection between magnetic fields in jets in the hearts of AGNs with jets at the largest scales (1 kpc–1 Mpc). We conclude our study with a discussion of future prospects in this field (Section 5).

2 Magnetic launching of jets

2.1 Observed properties of protostellar jets

Observations of the launch regions even of protostellar jets face significant observational challenges. For the nearest regions of star formation and jets in the Taurus molecular cloud (distance 140 pc), $1''$ resolution corresponds to a physical scale of 140 AU. Theoretical

models discussed below picture a jet acceleration region which is of the order of several tens of AU ($0.1''$), and the launch region in the very inner regions of the disc (several AU) that may be an order of magnitude smaller ($0.01''$). Jets around young stars have been studied on scales ranging from tens of AU to 5 pc (Bally et al. 2007).

Hubble Space Telescope (*HST*) observations of jets from YSOs have advanced our experimental understanding of jets enormously over the last decade, probing physical scales down to tens of AU. There are four basic types of observations that point towards the strong coupling of jets with underlying accretion discs — the correlation of jets with discs, the onion-like velocity structure of jets, jet rotation, and the strong link between the rates of mass transport in the jet to the accretion rate in the underlying disc. The advent of high resolution, spectro-imaging of jets by the *HST* and ground-based observatories equipped with adaptive optics has revealed their remarkable internal structure. Jets are strongly correlated with the presence of protostellar accretion discs around their host stars — at least during the first million years or so of their pre-main sequence evolution. Protostellar jet properties can be directly probed by observations of the forbidden line emission that they produce. Optical forbidden lines of oxygen, sulphur and nitrogen, for example, are produced in very specific ranges of density and temperature (see Ray et al. 2007, for a review). The spectro-imaging results indicate that jets have an "onion-like" velocity structure, with the highest-speed outflow component, up to 400 km s^{-1} in some sources, found at the core of the jet, while the lower-velocity components are found systematically farther from the outflow axis. The highest-resolution (*HST*) studies of the launch region of TTS jets (about 50 AU) show gas densities $> 2 \times 10^4$ cm^{-3}, modest electron temperatures ($T \simeq 2 \times 10^4$ K), and low ionization levels ($0.03 - 0.3$) (Coffey et al. 2008). As we shall see, the onion-like velocity structure seen close to the source is a reflection of the differential rotation of the underlying Keplerian disc. Higher-resolution observations, down to the 1-AU scales predicted for jet launch, would be highly desirable.

The discovery of jet rotation is perhaps one the most significant advances of the last decade (Bacciotti et al. 2002; Coffey et al. 2004). By orienting the slit of the spectrograph perpendicular to the jet axis at some distance along the jet, velocity asymmetry that is compatible with jet rotation can be observed. Shifts range from 5-25 km s^{-1} at positions of 25 AU along the jet. From the point of view of jet dynamics, these observations allow one to measure the amount of angular momentum that is being carried by the jet — which ranges from $\sim 60\%$ to $\sim 100\%$ of the angular momentum that would be carried through the disc by the observed disc accretion rates. The ratio of mass carried in the jet to that moving through the underlying accretion disc, $\dot{M}_{jet}/\dot{M}_a \simeq 0.01 - 0.07$ (Coffey et al. 2008).

The strength of the magnetic field in the HH80-81 jet is estimated from the synchrotron emission (on the basis of equipartition arguments: see Section 4.2), to be 0.2 milligauss (Carrasco-González et al. 2010). Even though the temperatures of jets are quite low, the mechanism of diffusive shock acceleration has been shown to be able to accelerate electrons moving at a few hundred km s^{-1} up to relativistic speeds. If this technique can be exploited, we may indeed be on the threshold of being able to measure all of the basic physical quantities that are needed to test the physics of protostellar jets.

2.2 Structure and dynamics of non-relativistic jets

At the heart of the question of why jets are ubiquitous is the fact that rapidly rotating magnetized bodies undergo strong spin-down torques exerted by the threading fields. The basic theory of magnetized winds from rapidly rotating stars was first worked out in the seminal

paper by Mestel (1968). This theory focuses on stationary solutions of axisymmetric flows from magnetized bodies — as applied in particular to rotating stars. It has turned out that this theoretical framework is very useful in analyzing the structure of jets and of the structure of their magnetic fields.

The overall dynamics of jets, and the physics of how they are launched, is complicated. However, significant progress has been made by the application of the theory of stationary, 2D (axisymmetric) MHD flows. The usefulness of this highly simplified treatment arises from the fact that we can derive conservation laws that turn out to be important even for understanding the behaviour of stationary jets in 3D. First we decompose vector quantities into poloidal and toroidal components (e.g. magnetic field $\mathbf{B} = \mathbf{B_p} + B_\phi \hat{\mathbf{e}}_\phi$). In axisymmetric conditions, the poloidal field $\mathbf{B_p}$ can be derived from a single scalar potential $a(r, z)$ whose individual values, $a =$ const, define the surfaces of constant magnetic flux in the outflow and can be specified at the surface of the disc (Pelletier and Pudritz 1992).

The joint conservation of mass and magnetic flux along a field line can be combined into a single function k that is called the "mass load" of the wind, which is a constant along a magnetic field line:

$$\rho \mathbf{v_p} = k \mathbf{B_p}. \tag{1}$$

This function represents the mass load per unit time, per unit magnetic flux of the wind. For axisymmetric flows, its value is preserved on each ring of field lines emanating from the accretion disc. Its value on each field line is determined by physical conditions — including dissipative processes — near the surface of the rotor.

The mass load plays a central role in jet dynamics (see Sections 3 and 4) and controls jet rotation, collimation, and angular momentum extraction. It may be more revealingly written as

$$k(a) = \frac{\rho v_p}{B_p} = \frac{d\dot{M}_\mathrm{w}}{d\Psi}, \tag{2}$$

where $d\dot{M}_\mathrm{w}$ is the mass flow rate through an annulus of cross-sectional area dA through the wind and $d\Psi$ is the amount of poloidal magnetic flux threading through this same annulus. The mass load profile (as a function of the footpoint radius r_0 of the wind on the disc) is determined by the physics of the underlying disc and imposes an important boundary condition for all aspects of jet physics.

The conservation of angular momentum along each field line leads to the conserved angular momentum per unit mass;

$$l(a) = r v_\phi - \frac{r B_\phi}{4\pi k} = \text{const}. \tag{3}$$

The form for l reveals that the total angular momentum is carried by both the rotating gas (first term) as well by the twisted field (second term), the relative proportion being determined by the mass load.

The value of $l(a)$ that is transported along each field line is fixed by the position of the Alfvén point in the flow, where the poloidal flow speed reaches the Alfvén speed for the first time ($m_\mathrm{A} = 1$). Hence, the value of the specific angular momentum is found to be

$$l(a) = \Omega_0 r_\mathrm{A}^2 = (r_\mathrm{A}/r_0)^2 l_0. \tag{4}$$

where $l_0 = v_{K,0} r_0 = \Omega_0 r_0^2$ is the specific angular momentum of a Keplerian disc. (Note, however, that this treatment can easily be generalized to sub-Keplerian discs.) For a field line starting at a point r_0 on the rotor (disc in our case), the Alfvén radius is $r_\mathrm{A}(r_0)$ and this constitutes a lever arm for the flow. The result shows that the angular momentum per

unit mass that is being extracted from the disc by the outflow is a factor of $(r_{\rm A}/r_0)^2$ greater than it is for gas in the disc. For typical lever arms, one particle in the outflow can carry the angular momentum of ten of its fellows left behind in the disc.

The conservation of energy along a field line is expressed as a generalized version of Bernoulli's theorem. Since the terminal speed $v_p = v_\infty$ of the wind is much greater than its rotational speed, and for cold flows, the pressure may also be ignored, one finds the result:

$$v_\infty \simeq 2^{1/2}\Omega_0 r_{\rm A} = (r_{\rm A}/r_0)v_{\rm esc,0}. \tag{5}$$

There are several important consequences for jet dynamics that follow from this simple scaling. The first is that the terminal speed exceeds the *local* escape speed from its launch point on an accretion disc by the lever arm ratio. Furthermore, the scaling predicts that the terminal speed scales with the Kepler speed as a function of radius, so that the flow will have an onion-like layering of velocities, with the largest velocities inside and the smallest on larger scales. As we have already noted, such velocity structure is actually observed in the dynamical structure of well-resolved jets. Finally, the terminal speed depends on the depth of the local gravitational well at the footpoint of the flow (the dependence on the local Keplerian rotation speed in the case of a disc rotor) — implying that it is essentially scalable to flows from discs around YSOs of any mass and therefore universal.

2.3 Determining the jet launch region

A very useful combination of the energy and angular momentum conservation that we derived above is given by the Jacobi constant along a field line (e.g., Pelletier and Pudritz 1992); $j(a) \equiv e(a) - \Omega_0 l(a)$. This expression has been used (Anderson et al. 2003) to constrain the launch region on the underlying Keplerian disc. Observers measure the jet rotation speed, $v_{\phi,\infty}$ at a radius r_∞, and the poloidal speed of the jet at this point, $v_{p,\infty}$. Evaluating j for a cold jet at infinity and noting that its value (calculated at the foot point) is $j(a_0) = -(3/2)v_{\rm K,0}^2$, one can solve for the Kepler rotation at the point on the disc where this flow was launched:

$$\Omega_0 \simeq v_{p,\infty}^2 / \left(2v_{\phi,\infty}r_\infty\right). \tag{6}$$

When this relation is applied to the observed rotation of the Large Velocity Component (LVC) of the jet DG Tau (Bacciotti et al. 2002), this yields a range of disc radii for the observed rotating material in the range of disc radii, 0.3–4 AU, and the magnetic lever arm is $r_{\rm A}/r_0 \simeq 1.8$–2.6. These results show that an extended region of the disc can give rise to the jet, and that, moreover, the lever arm is in the predicted range for the efficient launching of jets.

2.4 The disc/jet connection: magnetic torques on discs

The magnetized wind that is accelerated off the rotor carries away the rotor's angular momentum. In the case of an accretion disc, the angular momentum equation for the accretion disc undergoing a purely external magnetic torque (i.e., viscous torque neglected) may be written:

$$\dot{M}_{\rm a}\frac{d(r_0 v_0)}{dr_0} = -r_0^2 B_\phi B_z|_{r_0,H}, \tag{7}$$

where we have ignored transport by MRI turbulence or spiral waves. Note that the toroidal field plays a fundamental role in disc structure and accretion because it is so central to the

action of a magnetic torque upon the disc. By using the relation between the poloidal field and outflow on the one hand, as well as the link between the toroidal field and rotation of the disc on the other, the angular momentum equation for the disc yields one of the most profound scaling relations in disc wind theory, namely, the link between disc accretion and mass outflow rate:

$$\dot{M}_{\rm a} \simeq (r_{\rm A}/r_0)^2 \dot{M}_{\rm w}. \tag{8}$$

The observationally well-known result that, in many systems, $\dot{M}_{\rm w}/\dot{M}_{\rm a} \simeq 0.1$ is a consequence of the fact that lever arms are often found in numerical and theoretical work to be $r_{\rm A}/r_0 \simeq 3$ – the observations of DG Tau being a perfect example. Finally, we note that the angular momentum that is observed to be carried by these rotating flows (e.g., in DG Tau) is a consistent fraction of the excess disc angular momentum – from 60–100% (Bacciotti et al. 2004), which is consistent with the high extraction efficiency discussed here.

In reality, the evolution of discs is dictated by both viscous as well as wind torques. The magnetic torque exerted on the underlying disc has important effects upon its structure (Ferreira 2002; Ferreira and Casse 2004). Compared to standard α-disk models, Combet and Ferreira (2008) show that outflow torques modify the underlying radial structure of discs, resulting in column density jumps of a couple of orders of magnitude in going from the outer SAD solution to the inner-jet dominated zone of the disc. The jet-dominated region is also cooler and thinner.

2.5 Jet collimation and toroidal fields

In the standard picture of hydromagnetic winds, collimation of an outflow occurs because of the increasing toroidal magnetic field in the flow resulting from the inertia of the gas. Beyond the Alfvén surface, the ratio of the toroidal field to the poloidal field in the jet is of the order $B_\phi/B_p \simeq r/r_{\rm A} \gg 1$, so that the field becomes highly toroidal beyond the Alfvén surface. Collimation is achieved by the tension force associated with the toroidal field which leads to a radially inwards directed component of the Lorentz force (or "z-pinch"); $F_{\rm Lorentz,r} \simeq j_z B_\phi$.

The current carried by a jet can be easily written down:

$$I = 2\pi \int_0^r j_z(r', z') dr' = (c/2) r B_\phi. \tag{9}$$

The link between magnetic field structure and the collimation of jets was made by Heyvaerts and Norman (1989), where it was shown that two types of solution are possible, depending upon the asymptotic behaviour of the total current intensity in the jet. In the limit that $I \to 0$ as $r \to \infty$, the field lines are paraboloids which fill space. On the other hand, if the current is finite in this limit, then the flow is collimated to cylinders. The collimation of a jet therefore depends upon its current distribution — and hence on the radial distribution of its toroidal field.

It can be shown (Pudritz et al. 2006) that, for a power-law distribution of the magnetic field in the disc, $B_z(r_0, 0) \propto r_0^{\mu-1}$, with an injection speed at the base of a (polytropic) corona that scales as the Kepler speed, that the mass load takes the form $k \propto r_0^{-(1+\mu)}$. In this regime, the current takes the form $I(r, z) \propto r_0^{-(\mu+1/2)}$. Thus, the current goes to zero for models with $\mu < -1/2$, and these therefore must be wide angle flows. For models with $\mu > -1/2$, however, the current diverges, and the flow should collimate to cylinders.

These results predict that jets should show different degrees of collimation, depending on how they are mass loaded. As an example, neither the highly centrally concentrated, magnetic field lines associated with the initial split-monopole magnetic configuration used in simulations by Romanova et al. (1997), nor the similar field structure invoked in the X-wind model (Shu et al. 2000) should become collimated in this picture. On the other hand, less centrally (radially) concentrated magnetic configurations such as the potential configuration of Ouyed and Pudritz (1997) and Blandford and Payne (1982) should collimate to cylinders. By varying both the density profile of the disc as well as its magnetic structure, Fendt (2006) showed simulations in which highly collimated outflows from a "flat" radial disk structure produced unsteady knots in the jet.

The magnetic collimation picture, although it has considerable support from theory and simulations, has been questioned by Spruit (2010), who notes that the toroidal magnetic pressure in jets will force them to expand. Collimation in this picture results from magnetic fields and pressure in the external medium. Simulations do indeed provide evidence for a regime in which magnetic bubbles associated with simulations of protostellar outflows are observed to expand radially. These cases arise in simulations of disc winds that produce weak toroidal jet fields (Seifried et al. 2012). Strong toroidal fields in these jets give rise to well collimated flows.

2.6 Computer simulations: magnetic field structure of jets and their stability

Numerical simulations have played an enormous role in exploring the origin and evolution of jets. The pioneering stage of simulations of jets from discs took place in the mid 1980s through the 1990s, with the advent of magnetohydrodynamics (MHD) codes such as ZEUS. These early simulations recognized that, since the mass load of the disc outflow is a key variable that controls jet dynamics and structure, then the disc can be taken as a boundary condition for the flow, with the initial magnetic field structure and mass loading defined across this boundary. Simulations demonstrated most aspects of the theory outlined above — the collimation of the jet, the concentration of jet density towards the axis of the flow, the acceleration to high speeds, the "onion-like" velocity structure of the jet, and the dominance of the toroidal magnetic field structure can be seen (e.g., Ouyed et al. 1997; Ouyed and Pudritz 1997; Romanova et al. 1997; Krasnopolsky et al. 1999; Fendt 2006). Highly episodic behaviour of jets arises as a consequence of sufficiently low mass loading of the jets (Ouyed et al. 1997).

Figure 1 shows ZEUS 3D simulations of a jet being launched from an underlying disc (Staff et al. 2010). The two panels show snapshots of the magnetic field line geometry and jet density that arises within two particular jet models — those of Ouyed and Pudritz (1997) and Blandford and Payne (1982). The field lines have a distinct toroidal component that dominates the structure of the overall field on larger scales. Poloidal magnetic field dominates towards the axis of the outflow. The bow shock created by the jet is clearly seen in both cases. The general structure of these models is rather similar. The densest part of the jet are surrounded by a diffuse cavity-like region that is dominated by the toroidal magnetic field. The more extended outer material moves more slowly than the jet core.

If jets are dominated by toroidal fields far from the jet axis, why are they stable? Theoretical studies of the linear stability of jets show that they should become unstable when their speeds exceed the local Alfvén velocity (Ray 1981). This was further demonstrated by 3D simulations of idealized radio jets by Hardee and Rosen (1999). It turns out, however, that toroidally dominated jets stabilize themselves through nonlinear processes. Simulations

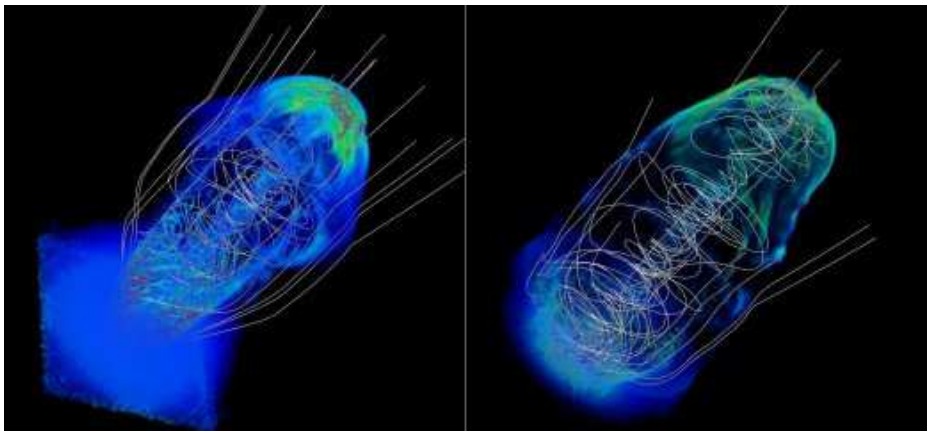

Fig. 1 Density and magnetic field lines for the Ouyed and Pudritz (1997) and Blandford and Payne (1982) models for the distribution of disc magnetic fields. The snapshots are shown as the jets have propagated out to 60 AU in the medium surrounding the magnetized disc. The protostar and the accretion disc are in the lower left corners of the panels, and hidden by the dense disc corona. Note that the core of the jet is dominated by poloidal field lines, while the outer regions are predominantly toroidal. Adapted from Staff et al. (2010).

show that jet instability, particularly in the form of $m = 1$ helical modes, builds up beyond the Alfvén surface(Ouyed et al. 2003). These are stabilized by the magnetic tension that stretches field in the linearly unstable region, which ultimately increases the local Alfvén speed again. The net result is a jet that is non-linearly stabilized by this mechanism, as well as by the "backbone" provided by the poloidal field that dominates near the outflow axis.

Since jets and accretion discs are highly coupled, jet torque and evolution will directly affect the disc. Hence, there has been a major effort over the last decade to simulate jets and their discs as a single dynamical system (e.g., Kudoh et al. 2002; Casse and Keppens 2002; von Rekowski and Brandenburg 2004). The important advantage of this approach is that one can avoid *ad hoc* descriptions of the mass loading and disc magnetic field line structure since these are self-consistently computed. These simulations show that jet structure and dynamics retain the basic features that the simpler simulations capture. Moreover, simulations by Zanni et al. (2007) which include the disk, and follow the evolution of jets using the Adaptive Mesh Refinement code FLASH, find that more than 90% of the gravitational potential energy liberated in the accretion flow is released into the jet. Thus jets are highly efficient in extracting both energy and angular momentum from the underlying accreting systems.

2.7 Jets from magnetized star-disc systems

So far we have emphasized disks as the underlying magnetized engines for jets. However, collimated outflows may derive from both the central stars as well as their surrounding disks. T-Tauri stars (TTS) are well known to be significantly magnetized (Johns-Krull 2007). As evidence that this may be occurring, we focus on the fact that TTS are also known to rotate very slowly for the amount of angular momentum that they are known to be accreting. This has long been known to imply that there must be some external torque being exerted upon the rotating star, carrying off or intercepting the angular momentum. It has been proposed that this torque takes the form of an interaction of the star's magnetosphere and the surrounding disk through closed magnetic field lines (Königl 1991). Recent work suggests that

most of the field in such interaction is readily opened up by shear in the disk, leading to very little spin-down torque and connection between star and disk (e.g.. Matt and Pudritz (2004). The interaction between inner disk and stellar magnetosphere has also been hypothesized to give rise to a so-called "X-wind", wherein the origin of jets and outflows is pictured to be an MHD outflow — based on the principles we discussed above — and originating from the very inner edge of the disk (Shu et al. 2000). In this picture, dipolar stellar magnetic field lines interacting with the inner edge of the disc are opened, leading to an outflow which intercepts angular momentum flowing inwards through the disc and driving it out of the system in the outflow. One difficulty with this models is in accounting for the huge amount of angular momentum that jets are observed to transport — 60% or more of the angular momentum transport through the disc at scales of 2 AU or so (Coffey et al. 2008); another issue is the difference between observed magnetic field strengths and the field strengths needed to drive the X-winds (Johns-Krull 2007). A third class of models has been proposed, wherein an accretion-powered wind from a magnetized, central star carries off the disk angular momentum (Matt and Pudritz 2005). The energy driving this wind is ultimately drawn from the gravitational energy that is released by the infalling material from the disc as it falls along magnetospheric field lines connecting the star and the disc. A strong flux of Alfvén waves stimulated by the impact of the accretion flow upon the star creates a wave-driven wind (Matt and Pudritz 2005, 2008; Cranmer 2008).

Simulations of such combined magnetized star-disk systems have been carried out in which both the central rotating magnetized star and the surrounding disk are treated as boundary conditions for the flows (Fendt 2009). Compared to the case of pure disk winds, the overall outflow is initially less collimated. This changes with time, however, as a highly collimated flow emerges as a new dynamical state across the grid when a stellar wind is included. The magnetic interaction between the two wind components gives rise to reconnection and large-scale flares as well, and the time-scale for the flaring is long — of the order of hundreds of inner disc rotation periods. Finally, if the outflow is dominated by the stellar wind, the outflow is either too weak or too high for low and high mass loads respectively. The disk jet is required to have stable collimated flow out to large scales.

The interaction of spinning, magnetized stars with their surrounding disks have been extensively simulated for axisymmetric configurations (Romanova et al. 2002; Bessolaz et al. 2008). Magnetospheric accretion has been likened to "funnel flow" wherein matter falls onto the star along field lines that are connected to the star and co-rotate with it. The matter moves due to the gravitational force, which dominates over the centrifugal force. The lifting of material off of the disc and the onset of the funnel flow starts at the radius at which the disk is slowed due to interaction with the more slowly spinning magnetosphere. These simulations showed that the interaction is time-dependent, with bursts of accretion followed by quiescent periods in which material from the disc piles up against the magnetosphere. Models usually assume that the disks are characterized by a model "α-disc" viscosity. In self-consistent 3D simulations, accretion flow from a turbulent disk onto a tilted magnetized star, where turbulence is driven by the MRI instability, has been modelled (Romanova et al. 2012). The pattern of alternating compression due to accretion and reconnection is also seen in these 3D simulations. The magnetosphere truncates the disk at a few stellar radii. The magnetic structure of the disk outside of the stellar magnetosphere has a toroidal field B_ϕ that is a few times larger than the poloidal field component. As we have noted several times, the transport of angular momentum by twisted field lines is an important part of the outflow mechanism. In the star-disc interaction, the magnetic stresses dominate the matter stresses in the disk and the pattern is quite inhomogeneus. This goes together well with the predictions outlined in the basic theory above. Finally, recent simulations of star-disc systems report the

launch of fast outflow at the interface in systems undergoing very high accretion rates — wherein the magnetic field in the star is strongly compressed (Lii et al. 2012). No X-winds are observed for the much lower accretion rates that dominate most of the star's accretion (Bessolaz et al. 2008).

2.8 Discs and jet formation during gravitational collapse

We now leave the domain of stationary outflows, and examine how they arise in the fully dynamical environments that characterize the birth of stars. Protostellar jets appear during the earliest stages of star formation and are the first obvious manifestation that gravitational collapse and star formation are underway. No 3D simulations of purely hydrodynamic collapse show that sustained jets can be produced in collapsing systems. This may be why they were missed in early hydrodynamical simulations of star formation. Add a threading magnetic field, however, and the launch of energetic jets and outflows is readily observed. The formation and evolution of jets takes place in a few related phases: (i) the formation and early evolution of a rotating, magnetized dense core, which is usually found embedded within larger scale filaments within molecular clouds; (ii) the extraction of angular momentum from the rotating core by torsional Alfvén waves during the early formation and collapse stages, which significantly de-spins the core; (iii) the gravitational collapse of a magnetized core with the ensuing formation of a protostellar accretion disc; (iv) the creation and launch of an outflow from the disc as it forms; and (v) the accretion of the disc onto the central star and with it, the gradual disappearance of the jet.

An important measure of the magnetization of the magnetized core is given by the so-called mass-to-flux ratio, which is the ratio of the gravitational to the magnetic energy of the system. Systems with supercritical ratios (values greater than unity) cannot be supported against collapse by their threading fields. The ratio can be written as (Mouschovias 1976)

$$\mu = \frac{M_{\rm core}}{\Phi_{\rm core}} / \left(\frac{M}{\Phi}\right)_{\rm crit} = \frac{M_{\rm core}}{\int B_z dA} / \frac{0.13}{\sqrt{G}} \,. \tag{10}$$

A second parameter of importance is the ratio of the rotational to the thermal energy of the core, known as β_{rot}. The phase space spanned by these two parameters turns out to divide up the physical properties of discs.

During the gravitational collapse of magnetized cores, the magnetic field threading the region is wrapped up — much like a twisting rubber band. As this happens, an outward flow of torsional Alfvén waves is created which transports angular momentum. Analytic solutions of the braking torque that arises for idealized, disc-like rotors have been written down. These have been found to fit the early stages of simulations of the collapse of a magnetized, Bonner-Ebert sphere (Banerjee and Pudritz 2006). As the collapse picks up, the winding of the field becomes particularly strong at the accretion shock. It is from this region that the first strong aspects of outflow begins. Soon after this happens, an inner region of outflow is launched which is centrifugally driven.

For fields that are sufficiently supercritical, the magnetic braking can be so significant that the disc material is left rotating at significantly sub-Keplerian levels. This has raised the question of whether or not discs can even form in the reasonably magnetized environments that are found in regions of star formation (Hennebelle and Fromang 2008; Mellon and Li 2008). The results depend quite sensitively on the initial conditions chosen — i.e., the mass-to-flux ratio. At values of $\mu \simeq 2$ – 10 , the resulting systems are strongly affected. This

intriguing result points to the importance of having appropriate astrophysical initial conditions. Recent simulations that feature long-term evolution of discs using "sink" particles find that in fact a reasonably Keplerian initial disc can form during the long-term evolution of the collapse (Duffin et al., in preparation). A grid of models for the formation of massive stars shows that reasonably quickly rotating cores and lower magnetized cores produce Keplerian discs (Seifried et al. 2011).

Figure 2 shows a zoomed-in picture of the magnetic structure that arises in the collapse of a solar mass system of a low mass star formation (Duffin et al. 2012, in preparation). The jet produced in this simulation reaches out to the extent of the initial Bonner-Ebert sphere, of about 10^4 AU in diameter. The gravitational collapse has pulled in the field lines which thread the disc. A transient, large disc of 2000 AU in extent has formed, which ultimately fragments into a ring and an inner 100 AU scale disc within an outer disc rotation period. The innermost region of the disc is seen to warp, which is a consequence of the torques induced by the magnetized wind. The outflow, as a consequence, precesses with the warp in the disc. Precessing jets are common and the simulation represented in this image shows, for the first time, that magnetic fields can cause this behaviour.

The launch mechanism of the outflows during collapse is under some current debate. For low-mass star formation ($M_{\rm core} \sim 1 M_\odot$), the generation, evolution and properties of protostellar outflows have been studied in great detail over the last years (e.g., Banerjee and Pudritz 2006; Mellon and Li 2008; Hennebelle and Fromang 2008; Duffin and Pudritz 2009). The two basic mechanisms that have been discussed in the literature focus on whether the outflow is driven by centrifugal acceleration (Blandford and Payne 1982; Pudritz and Norman 1986; Pelletier and Pudritz 1992; Ferreira 1997) or by the pressure of the toroidal magnetic field that was wrapped up in the initial collapse (Lynden-Bell 1996, 2003). The second mechanism — known as a tower flow — is highly transient and does not lead to sustained outflow moving out from the source. It is based on the study of equilibria of highly wound magnetic structures. General energy theorems demonstrate that they form tall magnetic towers, the height of which grows with every turn at a velocity related to the circular velocity in the accretion disc. The pinch effect amplifies the magnetic pressures toward the axis of the towers.

A more generalized criterion for outflow in disc wind theory, assuming that the gas is not strictly co-rotating with the field, has recently been proposed (Seifried et al. 2012). This model shows that disc-wind theories can have acceleration mechanisms that are driven by centrifugal forces as well as toroidal fields. Both magnetic tower and disc-wind theories can be commonly understood as a consequence of the same disc-wind models. It is of particular interest that the MHD flow equations discussed above actually have two aspects to them. Close to the outflow axis, it may be shown that the toroidal field generation is not significant, and there the outflow is driven like a centrifuge. Farther away, however, a toroidal field component is inescapably produced. It can be shown that the pressure gradient associated with this contributes to pushing a continuous outflow from the outer regions of the disc.

The two regions of the jet may be seen in Fig. 3 where we compare the size of the region controlled by purely centrifugal effects with those arising from toroidal pressure gradients. This illustrates that magnetic fields in jets play different roles depending upon where they are found. The difference between these two snapshots is the region in the jet where gas is driven primarily by toroidal field gradients. Note that these dominate in the outer parts of the jet, whereas the centrifugal driving predominates in the region close to the jet axis.

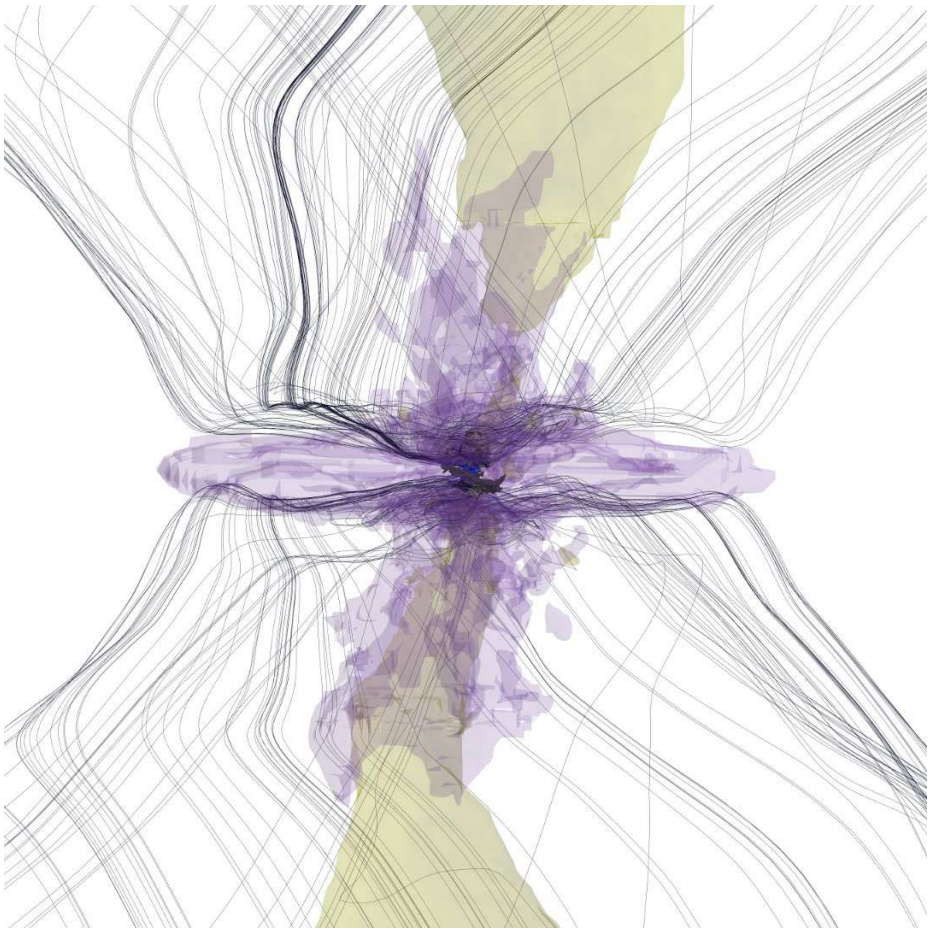

Fig. 2 Magnetic field structure in a collapsing magnetized core. A flattened structure is produced by the gravitational collapse. The purple contours correspond to 3.3×10^{-17} g cm^{-3} ($n = 8.5 \times 10^6$ cm^{-3}) and black contours to 1.3×10^{-15} g cm^{-3} ($n = 3.4 \times 10^8$ cm^{-3}). Yellow contours correspond to outflowing velocities $v_z > 1.5$ km s^{-1}, and extend to a height of 10^4 AU. Black lines are magnetic field lines. Adapted from Duffin et al. (2012).

2.9 Relativistic considerations and relation to protostellar jets

There is nothing in the physics of jets that suggests that relativistic sources, such as micro-quasars and AGN, and should have radically different driving mechanisms from those of protostellar systems — indeed, the dominant magnetic models make use of similar MHD equations. The fact that both a sufficiently rapidly rotating black hole and/or the surrounding magnetized disc are sources for relativistic jets has an obvious parallel with the protostellar systems. The theory and simulations of non-relativistic jets, as applied to protostellar systems, show some remarkable connections with the observations of AGN jets, which are discussed in Section 3 and Section 4. There are some important differences, however, which we discuss here.

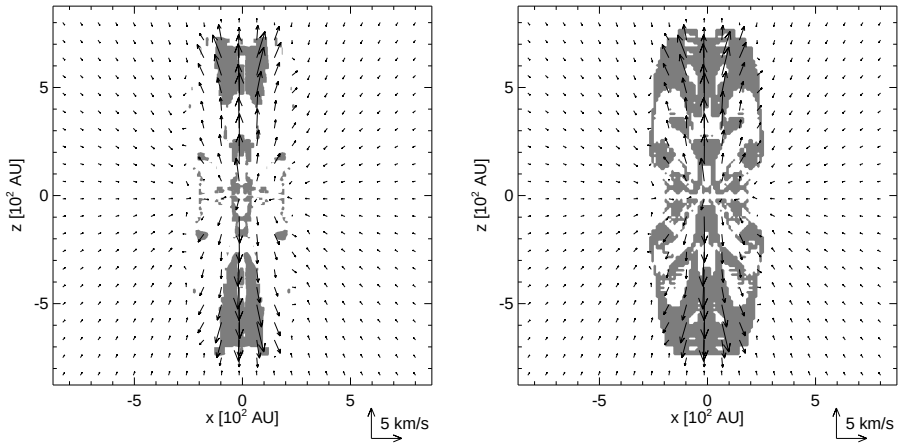

Fig. 3 Left: the region of jet that is driven by centrifugal acceleration — denoted in grey — in a simulation of a collapsing, solar mass, magnetized Bonner-Ebert sphere. Right: as left, but grey regions show the regions controlled by the full acceleration mechanism, including toroidal pressure gradients. Adapted from Duffin et al. (2012).

The theory of relativistic jets shows that the essential parameter is the *magnetization* parameter (Michel 1969; Camenzind 1986),

$$\sigma = \frac{\Psi^2 \Omega_{\rm F}^2}{4\dot{M}c^3}. \tag{11}$$

where the iso-rotation parameter $\Omega_{\rm F}$ is the angular velocity of the magnetic field lines. The function $\Psi = B_p r^2$ is a measure of the magnetic field distribution and $\dot{M} \equiv \pi \rho v_p R^2$ is the mass flow rate within the flux surface. Equation (11) demonstrates that the launch of a highly relativistic jet requires at least one of three conditions — rapid rotation, a strong magnetic field, and/or a comparatively low mass load. A strong magnetic field lowers the mass load in the jet, with the consequence that more Poynting flux can be converted into kinetic energy per unit mass flux.

In the case of a spherical outflow (Ψ = constant) with negligible gas pressure one may derive the Michel scaling between the asymptotic Lorentz factor and the flow magnetization (Michel 1969),

$$\Gamma_\infty = \sigma^{1/3} \tag{12}$$

Depending on the exact magnetic field distribution $\Psi(r, z)$, in a *collimating jet* the matter can be substantially accelerated beyond the fast magnetosonic point (Begelman and Li 1994; Fendt and Camenzind 1996). As a result, the power law index in eq. (12) can be different from the Michel-scaling (Fendt and Camenzind 1996; Vlahakis and Königl 2003).

An essential difference between relativistic and non-relativistic flows is the role of electric fields. They are negligible in non-relativistic flows but are comparable to magnetic fields in the relativistic case. The issue is that these fields can lead to the decollimation of the jet. Current-carrying relativistic jets have, however, been demonstrated to collimate (Chiueh et al. 1991). Relativistic jets have another feature with no counterpart in non-relativistic systems, namely the *light cylinder*, located at the cylindrical radius $r_{\rm l} = c/\Omega_{\rm F}$. At the light cylinder the velocity of the magnetic field lines "rotating" with angular velocity

$\Omega_{\rm F}$ coincides with the speed of light. Outside the light cylinder, the magnetic field lines "rotate" faster than the speed of light. As the field line is not a physical object, the laws of physics are not violated. The light cylinder is interpreted as the Alfvén surface in the limit of vanishing matter density (force-free limit). Crucially, *the location of the light cylinder determines the relativistic character of the magnetosphere. If the light cylinder is comparable to the dimensions of the object investigated, a relativistic treatment of MHD is required.*

Simulations of relativistic axisymmetric MHD disc winds have demonstrated that jets do indeed collimate, with half opening angles of 3–7° (Porth and Fendt 2010). These authors set up a relativistic analogue of the Ouyed and Pudritz (1997) simulations, and emphasized flows far enough away from the central black hole that general relativistic effects could be ignored. The outflow has a mixed character — a combination of the Blandford-Payne, centrifugally driven wind with a toroidal pressure-dominated flow of the type discussed by Lynden-Bell (1996). Lorentz factors of the order $\Gamma = 6$ are produced. The outflow has an interesting substructure, with a narrow relativistic jet towards the axis that is surrounded by a sub-relativistic flow launched from further out in the disc. This structure agrees with the observations of AGNs on the pc scales, as we discuss in Section 3. Finally we note that the toroidal fields that are generated in 3D simulations of jets seem to act as a sheath that protects the spine of the jet core from losing momentum to the surrounding medium (Mignone et al. 2010).

The advent of 3D general relativistic, MHD (GRMHD) codes (eg. McKinney (2006); McKinney et al. (2012)) has opened up the study of the role of black holes in the origin and evolution of AGN jets. As for the purely relativistic case, one of the primary questions is to determine how relativistic the jets become, and to understand what maintains their stability and collimation. It is generally thought that there are two regimes for AGN jets: a magnetized disk surrounding a black hole, as described by the Blandford and Payne (1982) picture, and/or the spinning black hole whose ergosphere is threaded by magnetic field, as originally envisaged by Blandford and Znajek (1977). Most theories and the simulations suggest that it is the spinning black hole that produces the highly relativistic jets, while lower-speed outflows arise from the surrounding disk. Recent GRMHD simulations (McKinney and Blandford 2009) model the initial threading magnetic field geometries for the spinning black hole as either a dipole or quadrupole configuration, while a thick torus is used to model an AGN disk. In addition to the need for significant spin of the central hole (the spin parameter of the hole is $a/M > 0.4$), their results demonstrate that the initial magnetic configuration also plays a significant role. Jets produced by an initial dipole structure can achieve high Lorentz factors, ($\Gamma > 10$) and remain highly collimated with an opening half-angle of $\theta_j \simeq 5^o$ at 10^3 gravitational radii. This is a stable jet with the substructure dominated by a stable $m = 1$ mode, probably excited in the underlying turbulent torus.

However, this does not occur for a more complex, quadrupolar, initial magnetic geometry, where the jet does not reach steady realistic speeds ($\Gamma < 3$). The quadrupolar field leads to mass loading which considerably slows the jet, and makes it prone to disruption. This outflow has a weak and disorganized poloidal field and a much stronger (by factor of 10-40) toroidal field. The authors speculate that these differences with the dipole jet may have something to do with the observed morphology of extragalactic jets; in particular, their classification into weakly relativistic "FR I-type" jets associated with AGNs in more clustered regions, and highly relativistic "FR II-type" jets associated with isolated objects. The latter would be associated with the spinning black holes and the former with the underlying accretion disks.

There are many similarities between these relativistic results and the non-relativistic work and theory described earlier. The stability of jets over a large variety of scales seems

assured for both regimes — they are able to run with stable substructure, dominated by an $m = 1$ mode, without falling apart. Both types of systems can remain very highly collimated, and this is related to their mass loading which is connected with their magnetic geometry. Moreover, toroidal magnetic field dominates the non-relativistic jet structure, which again is a likely consequence of the theory we have outlined in this Section.

In AGN systems, there is a concerted effort to understand jets on the smallest scales, which correspond to a few pc, in order to test theoretical models. The analysis described in this Section has shown that magnetic fields in jets are poloidal near the jet axis, and dominated by toroidal field farther out. This is a natural consequence of the acceleration and collimation mechanisms that should also apply to non-relativistic (eg. protostellar) and relativistic (AGN) accretion systems. We are now just beginning to be able to simulate the evolution of compact jets to larger scales (several pc) which allows direct comparison with observation. Simulations indicate that the field in protostellar jets becomes highly wrapped near the bow-shock of the jet (Staff et al. 2010), and this may have consequences for understanding AGN jets as well. In the next Section, we turn to the parsec-scale structure of AGN jets, to connect observations with the theory and simulations presented above.

3 Structure and dynamics of parsec-scale AGN jets

3.1 Backdrop for current studies

Radio studies of jets from Active Galactic Nuclei (AGNs) have primarily focused on parsec scales (with centimetre-wavelength Very Long Baseline Interferometry, VLBI, giving milliarcsecond resolution) and kiloparsec (kpc) scales (with arcsecond-resolution interferometers such as the Very Large Array and MERLIN), with relatively few observations probing intermediate scales. This means that, although the pc- and kpc-scale observations in some ways tell a coherent and self-consistent story, in others they seem to show discrepancies, with the connection between the behaviours observed on the two scales not always being clear. One reason for this may be that, although the parsec- and kpc-scale jets form different parts of a single structure, the observations may be determined by different contributions from “global” properties intrinsically related to the jet and “local” properties due to localized perturbations, interactions with the surrounding medium, variations in the magnetic field and density of the ambient medium, etc.

Throughout most of the period in which AGN jets have been studied with VLBI, since the early 1980’s, interpretations of observed features and behaviour have focused on the possibility that the observed jet properties are associated primarily with local agents, in particular, relativistic shocks propagating in the jets. From a certain point of view, this was very natural, and was motivated by factors such as the visibly inhomogeneous appearance of the jets themselves (they are often dominated by distinct components) and the common occurrence of variability. A theoretical framework arose in which the jet components were primarily shocks propagating along the jet, with various processes related to these shocks giving rise to the observed very rapid variability. This picture seemed to receive support from the earliest VLBI polarization observations, which showed that an appreciable number of AGN jet components have magnetic fields that are predominantly transverse to their jets — this was interpreted as reflecting the compression of an initially tangled magnetic field by a transverse shock, causing the field to become aligned in the plane of compression (Gabuzda et al. 1992).

More recently, various theoretical and observational studies have begun to explore the possibility that at least some of the polarization structures detected on parsec scales are associated with the intrinsic magnetic fields of the jets themselves. One area of such research involves theoretical simulations and observational searches for evidence of helical or toroidal magnetic fields carried by the jets, which are expected to form as aresult of the joint action of the rotation of the central black hole and its accretion disc and the jet outflow. The presence of toroidal or helical magnetic fields should give rise to characteristic transverse intensity and linear polarization structures across the jets, as well as transverse gradients in the observed Faraday rotation, due to the systematic change in the line-of-sight magnetic field across the jet.

Thus, one of the challenges currently faced by researchers studying AGN jets is to try to discern which features are primarily due to the action of local agents, such as shocks or interactions with the ambient medium, and which are primarily associated with the intrinsic magnetic field and other properties of the jets themselves. This Section will review recent observational results for high-resolution (VLBI) observations of AGN jets, together with some related theoretical simulations, in the framework of this challenge.

3.2 Estimates of VLBI-core B-field strengths

The direction of the magnetic field **B** giving rise to synchrotron radiation can be deduced from the direction of the associated observed electric vector position angle (EVPA), if the optical depth regime is known: in the absence of Faraday rotation, **B** is perpendicular to the EVPA in optically thin regions and parallel to the EVPA in sufficiently optically thick regions (see, e.g., Gabuzda and Gómez 2001). Thus, it is relatively straightforward to get an idea of the overall magnetic-field configuration even from VLBI observations at a single frequency, as long as the effects of Faraday rotation are not too severe. However, it is not possible to estimate the strength of the synchrotron B field directly using observations at a single frequency: multi-frequency observations are required, and even then, somewhat indirect techniques must be applied.

One of these is based on the frequency dependence of the position of the observed VLBI core in a Blandford–Königl jet (Blandford and Konigl 1979). In this picture, the VLBI core is essentially like a photosphere, and corresponds to the surface where the optical depth τ is equal to unity. The position of this $\tau = 1$ surface is located further down the jet at lower frequencies: $r \propto \nu^{1/k_r}$, where r is distance from the jet base, ν is frequency and k_r is a parameter that, in general, depends on the spectral index and the laws for the decline of the electron density and magnetic field with distance from the central engine (Konigl 1981). In practice, the observed VLBI core includes emission from both the vicinity of this $\tau = 1$ surface and the innermost jet, but the essence of this basic theoretical picture holds. In contrast to the behaviour of the core region, optically thin regions — in other words, regions in the jet — are expected to coincide at different frequencies. By aligning optically thin regions observed simultaneously at different frequencies and deriving the relative positions of the observed VLBI cores, the resulting "core shifts" can be used to derive estimates of the core magnetic fields, if reasonable estimates for the Doppler factor, viewing angle and jet opening angle are available (Lobanov 1998). This technique has only been applied to a handful of objects, but results obtained so far seem to give similar results for the cores of different AGNs, indicating that $k_r \approx 1$ in most cases (which corresponds to conditions not far from equipartition) and typical B fields at a distance of 1 pc from the jet base of about 0.15 Gauss (O'Sullivan and Gabuzda 2009a). Although these estimates are somewhat

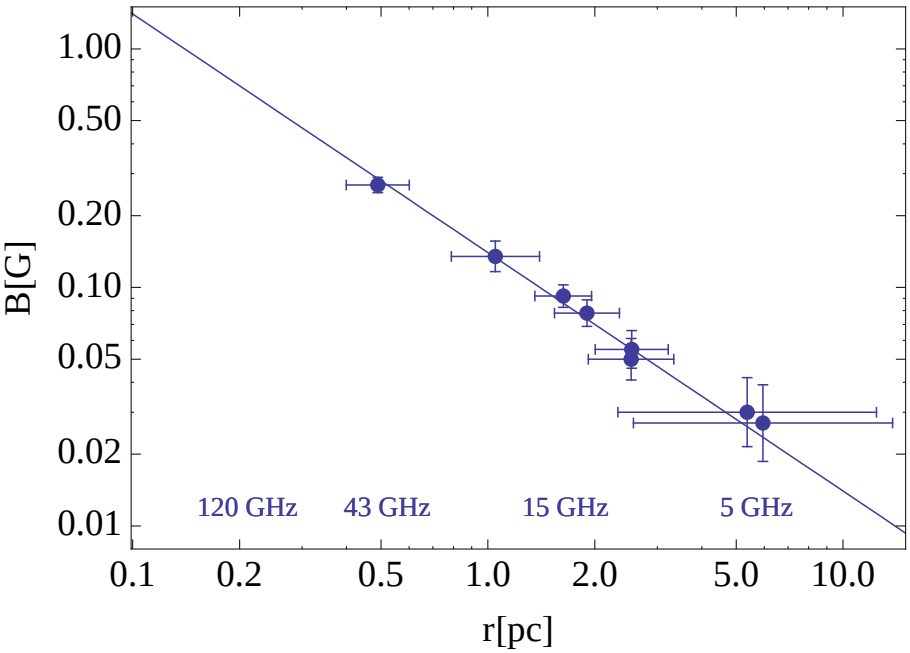

Fig. 4 Example of a derived dependence of B-field strength on distance from the jet base, approximately $B \propto r^{-1}$ (O'Sullivan and Gabuzda 2009a).

uncertain, due to uncertainties in the estimates of the Doppler factor and viewing angle, which cannot be derived directly from observations, the fact that similar core-region B fields are derived for various different AGNs suggests that these estimates are reasonably correct, at least to order of magnitude. These same studies have yielded evidence that the magnetic field falls off with distance from the jet base roughly as r^{-1} (Fig. 4).

3.3 Basic observational properties of the polarization of AGN jets

Although a wealth of polarization structure is observed among the variety of AGNs that have been studied with VLBI, it is possible to identify certain basic characteristics of the jet polarization. The most important of these is that, in a substantial majority of cases, the jet polarization is oriented close to parallel or perpendicular to the local jet direction (e.g., Lister and Homan 2005). The effect of Faraday rotation is usually modest outside the core regions, leading to polarization rotations of no more than $10 - 15^\circ$ at centimetre wavelengths (see also Section 3.5). For this reason, this tendency for the jet polarization to be either parallel or perpendicular to the local jet direction was evident even in the earliest VLBI polarization observations carried out at a single wavelength (e.g., Gabuzda et al. 1992; Cawthorne et al. 1993). On average, there is a tendency for AGNs with relatively luminous optical line emission ("quasars") to display higher apparent superluminal speeds and to most often have primarily longitudinal jet magnetic fields, while those having relatively weak optical line emission ("BL Lac objects") generally display lower apparent jet speeds

and most often have predominantly transverse jet magnetic fields (e.g., Gabuzda et al. 1994; Britzen et al. 2008).

Jet regions with oblique, or "misaligned", polarization (i.e., neither close to parallel or perpendicular to the local jet direction) that cannot be ascribed to Faraday rotation are sometimes observed, but are comparatively rare. Jets with extensive regions of longitudinal or transverse B field are observed. Little is known about the nature of "inter-knot" polarized emission located between bright jet features; VSOP space-VLBI polarization observations have revealed some cases in which longitudinal inter-knot polarization, implying transverse B fields associated with this underlying jet emission, are observed (Gabuzda 1999; Pushkarev et al. 2005).

Appreciable transverse polarization structure is observed in many jets, as becomes clear through a visual inspection of 15-GHz maps produced by the MOJAVE VLBA monitoring project (e.g., Lister and Homan 2005). In some cases, "spine+sheath" polarization structures are observed, with longitudinal polarization (orthogonal B field) near the central axis of the jet and orthogonal polarization (longitudinal B field) near the jet edges (e.g. Attridge et al. 1999; Pushkarev et al. 2005; Fig. 5). In other cases, the predominant polarization is orthogonal to the jet, and is offset appreciably from the central axis of the jet.

3.4 Interpretation of observations

Jet knots whose dominant polarization is longitudinal, implying a transverse B field, have frequently been interpreted as transverse shocks that have compressed an initially tangled magnetic field so that it has become ordered in the plane of compression (Laing 1980; Hughes et al. 1989), while the presence of orthogonal polarization (longitudinal B field) has been ascribed to the action of shear that has enhanced this component of the field in a layer surrounding the jet. Transverse polarization structures have similarly sometimes been interpreted as indicating the combined action of shocks and shear (e.g., Attridge et al. 1999). In the framework of the empirical connection between higher/lower apparent jet speeds and predominantly longitudinal/transverse jet magnetic fields, it has been suggested that transverse shocks may form more easily in jet outflows that have lower intrinsic speeds (Gabuzda et al. 1994; Duncan and Hughes 1994).

Alternately, all of these polarization structures can be understood as possible manifestations of helical magnetic fields carried by the jets (e.g., Lyutikov et al. 2005): for example, jets with predominantly orthogonal or longitudinal B fields could carry helical fields with relatively large or small pitch angles. The tendency for AGNs displaying higher/lower apparent superluminal speeds to be more likely to have primarily longitudinal/transverse jet magnetic fields is interesting in this connection. One possibility is that this could reflect a relationship between the pitch angle of a helical jet B field and the physical speed of the jet outflow: the ratio of the speed of the jet outflow to the rotational speed of the central black hole and accretion disc could be higher for quasars, leading to smaller pitch angles for the helical B fields threading their jets and a dominance of the longitudinal component of the helical field, whereas the low outflow speeds of BL Lac objects lead to higher pitch angles for their helical fields and a dominance of the toroidal component of the helical field.

The appearance of a "spine+sheath" transverse polarization structure or polarization, implying a longitudinal B field offset toward from the central axis of the jet, could likewise come about if the jet carries a helical magnetic field, with the azimuthal component dominating near the central axis of the jet and the longitudinal component becoming dominant near the edges. The different viewpoints advocated by these two different types of interpretation

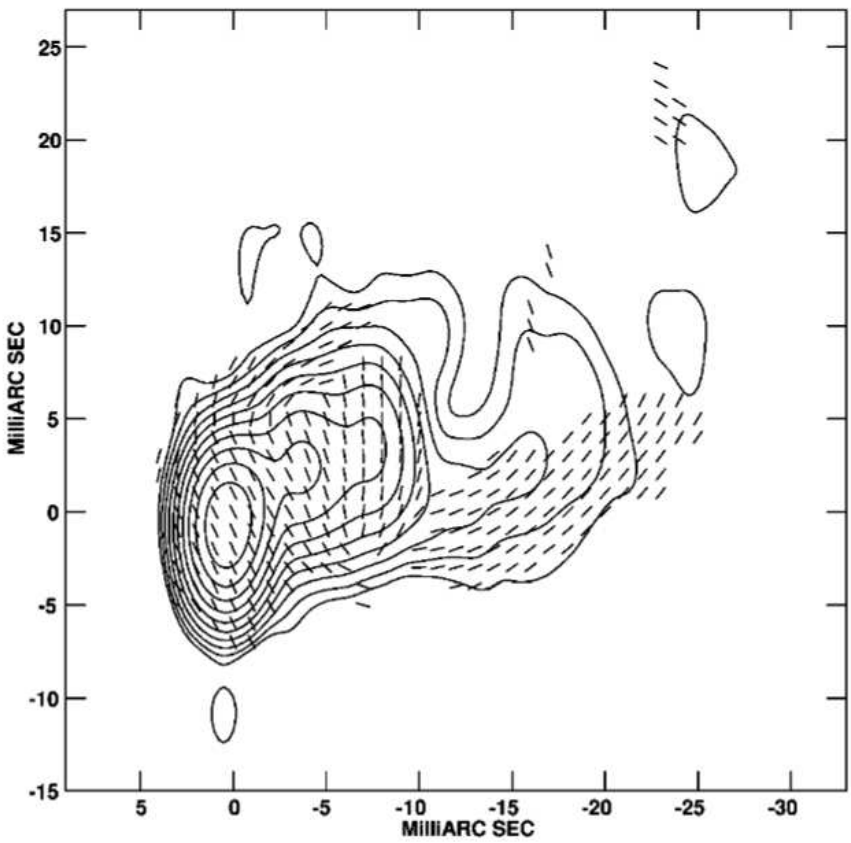

Fig. 5 Example of "spine+sheath" polarization structure across an the jet of the blazar 1055+018 (Attridge et al. 1999). The object is at a redshift $z = 0.888$, so 1 mas equals 7.78 pc. The vectors show the direction of the B-field.

essentially reflect the challenge referred to above, of distinguishing between characteristics associated with the action of local agents and those associated with intrinsic properties of the jets themselves.

Considerable progress has also been made recently in using the results of theoretical computations and simulations of AGN jets to generate simulated VLBI intensity, spectral-index, polarization and Faraday-rotation distributions that can, in principle, be compared with observations. Examples include the studies carried out by Zakamska et al. (2008), Gracia et al. (2009), Mimica et al. (2009), Broderick and McKinney (2010), Porth and Fendt (2010), Porth et al. (2011) and Clausen-Brown et al. (2011). Mimica et al. (2009) and Mimica & Aloy (2010, 2011) have considered various observational signatures of the presence of shocks and shock-heated gas in relativistic jets, including jets carrying helical fields. Broderick and McKinney (2010) and Porth et al. (2011) have generated theoretical Faraday-rotation images based on computations and simulations of AGN jets with a helical magnetic-field component. Porth et al. (2011) also considered the behaviour of the polarization angle as a function of the wavelength λ squared in the (partially) optically thick core region, demonstrating deviations from a λ^2 relation away from a limited range of relatively short

wavelengths; this effect appears to have been observed by O'Sullivan and Gabuzda (2009b). One limitation here is the need to use some scheme to extrapolate results for small scales to the scales accessible to observations with VLBI. However, such studies are beginning to enable much closer comparisons with observations than was possible previously, and are being used to identify a range of characteristic observational signatures of various types of jets and jet magnetic fields. It is clear that the ability to reliably measure transverse structure in intensity, spectral index, polarization and Faraday rotation across AGN jets will be key to probing the nature of the jet magnetic fields.

3.5 Observational evidence for helical or toroidal magnetic fields

As is discussed in Section 2 above, helical jet magnetic fields are predicted by a wide range of theoretical models and numerical simulations (e.g. Blandford and Payne 1982, Ouyed and Pudritz 1997, Krasnopolsky et al. 1999, Fendt 2006), making observational searches for evidence for helical magnetic fields associated with AGN jets of considerable interest. The most promising approach in this area is searching for transverse gradients in the Faraday rotation measure distribution across AGN jets, as was first pointed out by Blandford (1993). The observed Faraday rotation is proportional to the integral along the line of sight of $n_e\mathbf{B} \cdot d\mathbf{l}$, where n_e and $\mathbf{B}$ are the electron density and magnetic field in the region of Faraday rotation and the length element $d\mathbf{l}$ points along the line of sight toward the observer. Therefore, the magnitude of the Faraday rotation depends on the line-of-sight component of the ambient magnetic field, and the sign of the Faraday rotation is determined by the direction of this component of the field. Therefore, if a jet and its immediate vicinity are threaded by a helical magnetic field, this field will give rise to a systematic transverse gradient in the observed Faraday rotation, due to the systematic change in the line-of-sight component of the helical B field across the jet. The detection of such transverse Faraday-rotation gradients is observationally challenging, since it involves a joint analysis of multi-frequency radio images, and the observing conditions are not optimal on either parsec or kpc scales: on parsec scales, the jets are very compact, so that they are sometimes only marginally resolved in regions of strong polarization, even when observed with VLBI, while, on kpc scales, the jets are better resolved, but the effect is weaker due to the increased distance from the base of the jet. To obtain increased sensitivity to Faraday rotation, one can observe at longer wavelengths, however, this comes at the expense of a corresponding loss of resolution.

Nevertheless, firm detections of transverse Faraday rotation gradients have now been made for a number of AGNs. The first report of the detection of a transverse Faraday gradient across an AGN jet, interpreted as evidence for a helical jet B field, was made by Asada et al. (2002), based on Very Long Baseline Array (VLBA) observations of the nearby AGN 3C 273; this was later confirmed by Zavala and Taylor (2005), and the evolution of the gradient analyzed by Asada et al. (2008b). In the meantime, transverse Faraday-rotation gradients in several more objects were presented by Gabuzda et al. (2004). There have since then been at least ten further papers in refereed journals reporting the presence of transverse Faraday-rotation gradients across the jets of more than a dozen AGNs on parsec scales, interpreted as evidence that these jets carry helical magnetic fields (Asada et al. 2008b,2008a, 2010; Gabuzda et al. 2008; Gómez et al. 2008; O'Sullivan and Gabuzda 2009b; Kharb et al. 2009; Mahmud et al. 2009; Croke et al. 2010; Kronberg et al. 2011); one example is shown in Fig. 6. A number of other tentative cases have been presented in conference proceedings or identified in previously published Faraday-rotation images in the literature (e.g., Contopoulos et al. 2009; Zavala and Taylor 2003, 2004).

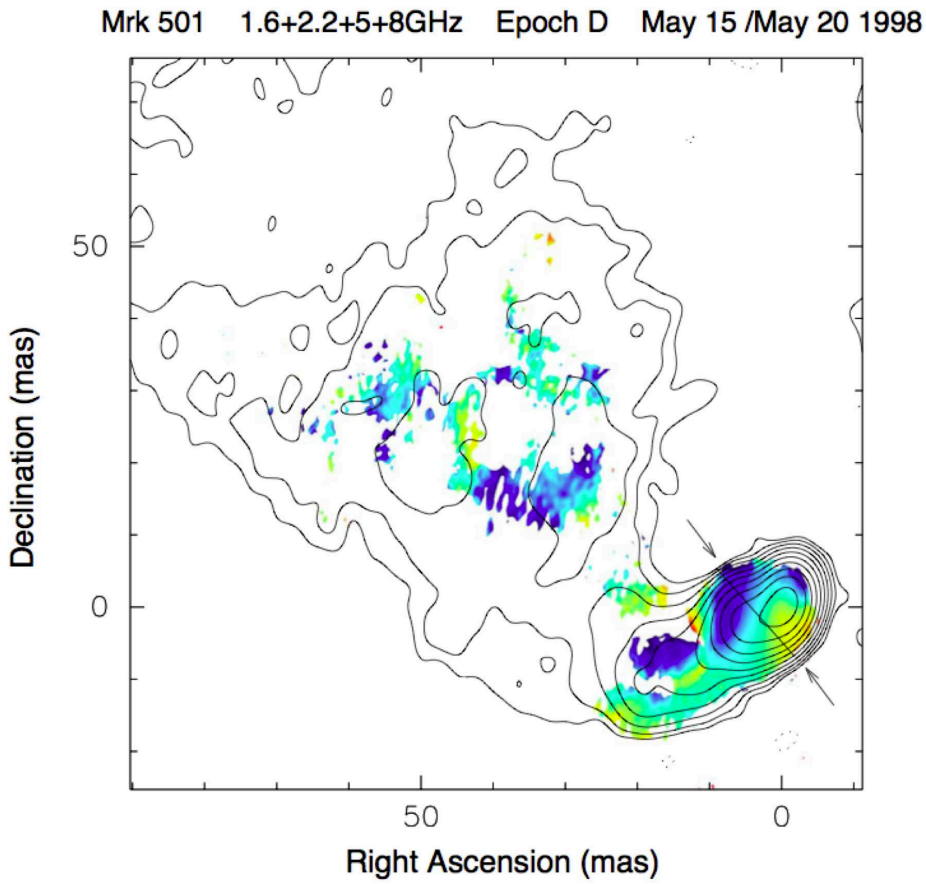

Fig. 6 Example of a transverse Faraday-rotation gradient detected across the jet of the blazar Mrk 501; the contours show the distribution of the radio intensity at 18cm, and the colour scale the distribution of the observed Faraday rotation (Croke et al. 2010). The redshift of this object is 0.034, so that 1 mas is 0.66 pc.

This suggests that, when the observing conditions enable their detection, transverse Faraday-rotation gradients across AGN jets are not uncommon on parsec scales. This result is potentially of crucial importance for our understanding of AGN jets, since it provides direct evidence that these jets carry helical magnetic fields, which, in turn, has obvious implications for the jet-launching mechanism. In addition, the presence of an appreciable ordered toroidal field component would imply that the jets carry current. It is therefore important to try to ensure that the requirements for the reliable detection of transverse Faraday-rotation gradients are well understood and applied.

It has sometimes been suggested that apparently transverse Faraday-rotation gradients could come about due to gradients in the ambient electron density, and therefore not have anything to do with the presence of a helical jet B field. An interesting point here is that, if the viewing angle of the jet in the jet rest frame is not too far from 90° (the jet is viewed roughly from the side in the jet rest frame), the observed Faraday rotation associated with the jet's helical field should change sign across the jet; if the jet viewing angle in the jet rest

frame is not close to 90°, the jet's helical field will still give rise to a transverse Faraday-rotation gradient, but there may not be a change in the sign of the Faraday rotation across the jet. Therefore, the clear detection of a change in the sign of the observed Faraday rotation across an AGN jet can easily be explained by the presence of a helical field, but not by electron-density gradients; such sign changes have been observed for a number of AGN jets (e.g., Asada et al. 2008a; Gabuzda et al. 2004, 2008; Mahmud et al. 2009).

Other observational problems that could potentially hinder the detection of transverse Faraday-rotation gradients associated with helical magnetic fields, or distort their interpretation, include the limited resolution available to centimeter-wavelength VLBI observations and optical depth effects in the region of the observed VLBI core (Taylor and Zavala 2010). The presence of non-monotonic and/or complex transverse Faraday-rotation gradients in the core region have been directly demonstrated by the simulations of Broderick and McKinney (2010) and Porth and Fendt (2010). These simulations indicate the difficulty of accurately deriving parameters of the jet and the helical field it is believed to carry based on observed transverse Faraday-rotation gradients. Note, however, that the direction of the simulated gradients is correct when they are monotonic; since most observational studies carried out thus far have focused on the detection of *monotonic* transverse gradients and their direction, the results of these studies are not greatly affected by the difficulties indicated by the simulation results.

Taylor and Zavala (2010) have proposed that a transverse Faraday-rotation gradient should span three "resolution elements" (taken to correspond to three beamwidths) in order for the gradient to be considered reliable; however, no theoretical basis was provided for this criterion. It is therefore of interest to develop more systematic and objective approaches to determining the resolution necessary to reliably distinguish transverse Faraday-rotation gradients, and results from a number of such studies have begun to appear. For example, Murphy and Gabuzda (2012) have calculated transverse intensity, polarization and Faraday-rotation distributions and subjected them to convolution with beams of various sizes. The initial results of these studies indicate that the detection of transverse polarization structure associated with helical jet B fields is much more robust to convolution with beams comparable to the jet width than is transverse intensity structure, although, of course, the convolution somewhat distorts the intrinsic polarization structure. Similarly, convolution of transverse Faraday-rotation gradients with beams that are comparable to or even larger than the transverse size of the jet reduces the magnitude of the Faraday-rotation gradient, but does not destroy the gradient completely. Hovatta et al. (2012) have recently presented the results of four-frequency VLBI polarization observations of roughly 200 AGNs, together with Monte Carlo simulations modeling the polarization uncertainties and how they are manifest in Faraday-rotation maps. These Monte Carlo simulations suggest that transverse Faraday-rotation gradients spanning as little as 1.5 beamwidths can be reliable, provided that the difference between the Faraday rotations on either side of the jet exceeds 3σ.

These results are also consistent with the general relativistic MHD simulations of Broderick and McKinney (2010), which directly demonstrate the presence of transverse Faraday-rotation gradients across regions that are only marginally resolved: transverse structures in their simulated Faraday-rotation distributions with intrinsic sizes less than 0.05 mas remain clearly visible even when convolved with a 0.9-mas beam. All this suggests that the minimum resolution required to reliably detect a transverse Faraday-rotation gradient across an AGN jet is considerably less than the three-beamwidth criterion suggested by Taylor and Zavala (2010), provided that the Faraday rotation measures measured on opposite sides of the jet can reliably be demonstrated to differ at more than the 3σ level. Of course, this concerns only the detection of the presence and direction of a transverse Faraday-rotation gradient; reli-

able measurement of the intrinsic magnitude of such a gradient would require much higher resolution.

Another issue that is currently being investigated is the question of how to accurately estimate the uncertainties at specific locations in VLBI images; this is non-trivial due to the complex computational procedures undertaken in the mapping process and the strong correlation between neighbouring pixels, due to convolution with the CLEAN beam. In the past, it has been usual to assign the uncertainty for a pixel in images of the Stokes parameters I, Q and U to be equal to the root-mean-square deviation about the mean calculated for a large region far from areas of source emission, but this is certainly an underestimate. Hovatta et al. (2012) and Mahmud et al. (2012) use Monte Carlo simulations to address this issue, motivated by the need to derive accurate estimates of uncertainties for individual locations in Faraday-rotation images.

Another interesting question in connection with the detection of transverse Faraday-rotation gradients across AGN jets is whether it is possible to observationally distinguish between a helical and a toroidal magnetic field. The point here is that the detection of the transverse gradient only demonstrates the presence of an ordered toroidal field component, without providing any information about the presence of a longitudinal field component. Both helical and toroidal jet B fields could give rise to "spine+sheath" transverse polarization structures, and a rise in the degree of polarization toward the edges of the jet, as is commonly observed. One means of distinguishing between these two possibilities is provided by the transverse intensity and polarization structure of the jet: a purely toroidal field can only produce symmetrical transverse intensity and polarization structures (e.g. Zakamska et al. 2008), whereas a helical field can produce either symmetrical or asymmetrical transverse structures, depending on the viewing angle of the jet and the pitch angle of the helical field (e.g., Murphy et al. 2010, 2012). Therefore, the joint detection of a transverse Faraday-rotation gradient and clearly asymmetrical transverse polarization structure would provide clear evidence for a helical, rather than a purely toroidal, jet B field.

Finally, note that Faraday rotation associated with detected transverse gradients observed can be external (not occurring throughout the radiating volume of the source), if it is associated with regions of helical magnetic field in the outer layers of the jet, or in the immediate vicinity of the jet.

3.6 Evidence for reversals in the direction of the toroidal field component

One of the most unexpected results to come out of recent parsec-scale Faraday-rotation studies is the detection of reversals in the direction of transverse Faraday-rotation gradients across AGN jets, both with distance from the base of the jet Mahmud and Gabuzda (2008); Hallahan and Gabuzda (2008); Mahmud et al. (2012) and with time (Mahmud et al. 2009). This is at first glance difficult to understand, since the direction of the observed Faraday-rotation gradient is determined by the direction of the toroidal field component, which is, in turn, essentially determined by the direction of rotation of the central black hole and accretion disc, together with the direction of the net poloidal component of the initial "seed" field that is wound up. It is not physically plausible for the direction of the system's rotation to change on measureable time scales, and changing the direction of the jet poloidal component of the seed field would seem to require a change in the polarity of the field of the black hole, which likewise, seems implausible, at last on measureable time scales. Bisnovatyi-Kogan (2007) has suggested the possiblity that, under certain circumstances, torsional oscillations can develop in a jet, which could give rise to changes in the direction of the toroidal B-field

component; in this scenario, the direction of the observed transverse Faraday-rotation gradients would reverse from time to time when the direction of the torsional oscillation reverses, and this reversal pattern would presumably then propagate outward with the jet.

However, Mahmud et al. (2009) and Mahmud et al. (2012) have suggested that a simpler and more likely explanation is a magnetic-tower-type model, with poloidal magnetic flux and poloidal current concentrated around the central axis (Lynden-Bell 1996; Nakamura et al. 2006). Fundamental physics dictates that the magnetic-field lines must close; in this picture, the magnetic field forms meridional loops that are anchored in the inner and outer parts of the accretion disc, which become twisted due to the differential rotation of the disc. This should essentially give rise to an "inner" helical B field near the jet axis and an "outer" helical field somewhat further from the jet axis. These two regions of helical field will give rise to oppositely directed Faraday-rotation gradients, and the total observed gradient will be determined by which region of helical field dominates the observed Faraday rotation. The presence of a change in the direction of the observed transverse Faraday-rotation gradient with distance from the jet base could represent a transition from dominance of the inner to dominance of the outer helical B fields in the total observed Faraday rotation. The reversals of the Faraday-rotation gradients with time observed for 1803+784 (Mahmud et al. 2009) could come about if the physical conditions in the jet changed such that there was a change in whether the inner or outer region of helical B field dominated the total observed Faraday rotation. If this interpretation is correct, these observations of reversals of the direction of transverse Faraday-rotation gradients across AGN jets represent the first observational evidence that the jet magnetic field closes in the outer accretion disc.

3.7 Evidence for the action of a cosmic battery

Any transverse Faraday-rotation gradient can be described as being directed either clockwise (CW) or counter-clockwise (CCW) on the sky, relative to the base of the jet. Contopoulos et al. (2009) have reported a significant excess of CW transverse Faraday-rotation gradients for parsec-scale AGN jets, based on transverse Faraday-rotation gradients identified in maps from the literature. Considering the gradient closest to the VLBI core if two distinct regions with transverse gradients were present (as is described in the previous subsection) yielded 29 transverse Faraday-rotation gradients on parsec scales, of which 22 were CW and only 7 CCW, with the probability of this coming about by chance being less than 1%. This is an extremely counterintuitive result, since the direction of the helical field threading an AGN jet should essentially be determined by the direction of rotation of the central black hole and accretion disc, together with the direction of the poloidal "seed" field that is wound up, and our instincts tell us that both of these should be random.

Contopoulos et al. (2009) suggest that this seemingly bizarre result can be explained in a straightforward way via the action of a mechanism they call the "Poynting–Robertson cosmic battery." The essence of this mechanism is the Poynting–Robertson drag experienced by charges in the accretion disc, which absorb energy emitted by the active nucleus and re-radiate this energy isotropically in their own rest frames. Because these charges are rotating with the accretion disc, this radiation will be beamed in the forward direction of their motion, i.e., in the direction of the disc rotation. Due to conservation of momentum, the charges then feel a reaction force opposite to the direction of their motion; since the magnitude of this force exhibits an inverse dependence on the mass of the charge, this leads to a difference in the deceleration experienced by the protons and electrons in the disc. Since the electrons are decelerated more strongly, this leads to a net current in the disc, in the direction of ro-

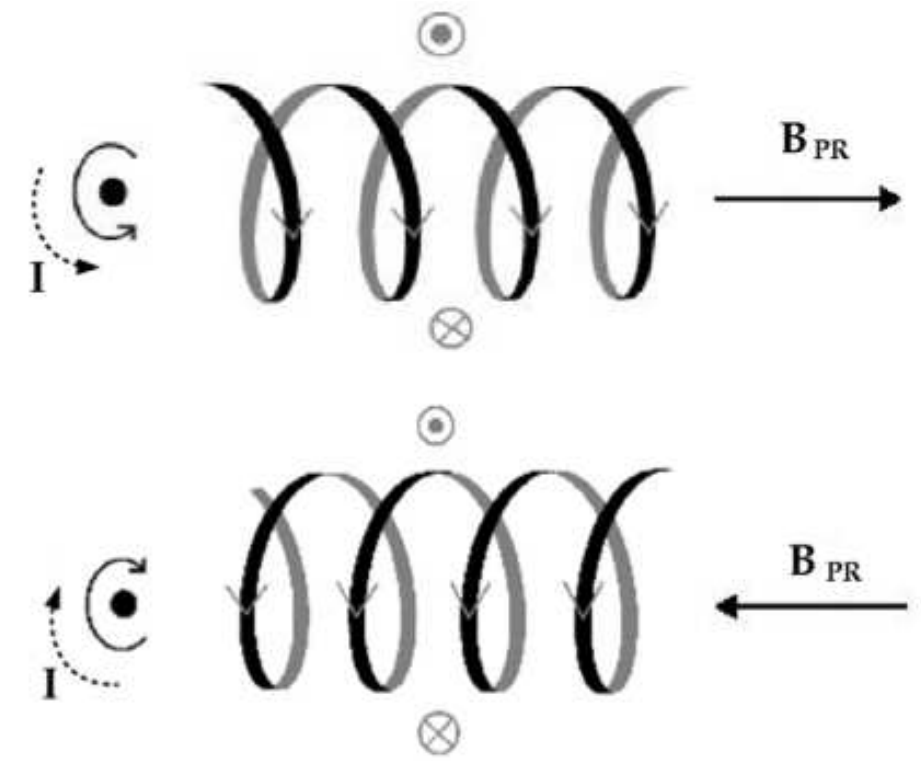

Fig. 7 Illustration of how the action of the Poynting–Robertson battery couples the direction of rotation of the accretion disc and the direction of the poloidal seed field that is wound up, leading to the creation of Faraday-rotation gradients associated with the resulting helical B field that are CW on the sky, independent of the direction of disc rotation (Mahmud 2010).

tation. This current, in turn, gives rise to a net poloidal magnetic field whose direction is coupled to the direction of the current in the disc, i.e., to the direction of the disc rotation. This coupling of the disc rotation and the direction of the poloidal field that is "wound up" breaks the symmetry in the direction of the toroidal field component, and predicts that the observed Faraday-rotation gradients should be predominantly CW on the sky, independent of the direction of the disc rotation as seen by the observer (Fig. 7). In a "nested helical field" type picture such as that described in the previous subsection, the inner/outer regions of helical field should give rise to CW/CCW Faraday-rotation gradients; therefore, the observed excess of CW implies that the inner region of helical B field dominates on parsec scales.

If this excess of CW Faraday-rotation gradients is confirmed by further studies, this will have cardinal implications for our understanding of AGN jets. The development of approaches to carrying out objective searches for reliable transverse Faraday-rotation gradients for as many AGNs as possible is of interest in this connection. Independent of the physical origin of the predominance of a particular orientation, the results of Contopoulos et al. (2009) essentially rule out the possibility that most of the observed gradients are spurious, and not associated with the toroidal field components of the jets, since spurious (incorrectly identified) gradients should certainly be randomly oriented on the sky. If the Poynting–

Robertson battery does not operate sufficiently efficiently to provide the observed excess of CW gradients, then some other mechanism that can couple the direction of rotation of the accretion disc and the direction of the poloidal field that is wound up by differential rotation must be identified.

3.8 Connection with kiloparsec scales

Recently, Christodoulou et al. (2012) (see also Gabuzda et al. 2012) searched the literature for transverse Faraday-rotation gradients across the kpc-scale jets and lobes of AGNs and radio galaxies. This yielded six AGNs displaying continuous, monotonic RM gradients across their jets, oriented roughly orthogonal to the local jet direction. The most fundamental implication of this result is that transverse Faraday-rotation gradients that can most naturally be interpreted as evidence for toroidal or helical magnetic fields threading the jets are also present on kpc scales. This is an important result, because, if the jets of AGNs carry helical magnetic fields, these should be present on essentially all scales where the jets propagate, provided that the intrinsic field structure of the jet is not disrupted by interactions with the surrounding environment.

Another intriguing aspect of the analysis of Christodoulou et al. (2012) is that all six of the firm transverse kpc-scale Faraday-rotation gradients identified are oriented CCW on the sky, relative to their jet bases. This is on the verge of being a firm result statistically: based on a simple unweighted binomial probability function, the probability for six out of six gradients to be CCW by chance is about 1.5%. However, the significance of this result is tentatively supported by VLBA observations of 3C 120 (Coughlan et al. 2010), Mrk501 (Croke et al. 2010), and 1749+701 (Hallahan and Gabuzda 2008): in each case, transverse CCW Faraday-rotation gradients are found on scales of tens of pc. Further, all AGNs for which reversals of their transverse Faraday-rotation gradients have been observed display CCW Faraday-rotation gradients further from the jet base (Mahmud and Gabuzda 2008; Mahmud et al. 2012; Reichstein and Gabuzda 2010; Coughlan et al. 2010). This growing evidence for a predominance of CW/CCW Faraday-rotation gradients on parsec/kpc scales can be interpreted as a consequence of a nested-helical-field configuration, as is described above, with the inner region of helical field dominating on parsec scales and the outer region of helical field dominating on kpc scales. This picture is consistent with theoretical studies of the jet launching mechanism (Blandford and Payne 1982; Contopoulos and Lovelace 1994; Contopoulos 1995; Spruit 2010), which suggest that the field is effectively wound up only beyond the Alfvén distance, which is $\sim$10 times the radial extent of the outflow at its base. Thus, the theoretical models suggest that the magnetic field in the inner jet and the outer extended accretion disc will develop significant toroidal components on distances beyond $\sim$10 AU and $\sim$10 pc, respectively, from the AGN centres; this would predict a predominance of CW Faraday-rotation gradients on observed scales less than $\sim$10 pc and of CCW gradients on scales greater than $\sim$10 pc, consistent with the results of Contopoulos et al. (2009) and Christodoulou et al. (2012). Thus, although the results of Christodoulou et al. (2012) must clearly be confirmed based on a larger number of AGNs, they have the potential to considerably influence our understanding of the overall magnetic-field configurations of AGN jets.

The analysis of Christodoulou et al. (2012) suggests that the occurrence of reliably detectable transverse Faraday-rotation gradients is appreciably lower on kpc than on parsec scales: they were able to find reasonably clear transverse Faraday-rotation gradients in only six of about 85 objects. In fact, this is quite natural. There is an appreciable turbulent, in-

homogeneous component to the thermal ambient media surrounding the jets on kpc scales, which superposes a more or less random pattern over the systematic pattern due to the helical fields (see the discussion in Section 4.3). This random component in the Faraday-rotation distribution may dominate in the majority of cases. Thus, it is natural that most of the observed Faraday-rotation distributions appear random and patchy, but the overall pattern due to the helical fields sometimes comes through. This suggests that, on average, it is easier to detect the systematic Faraday-rotation component due to helical jet magnetic fields on parsec scales, where the ordered inner field is more dominant.

The additional complications imposed by the large-scale interaction with the jet and the ambient medium, and the structures (lobes, hotspots etc.) generated by this interaction, are discussed in the following Section.

4 Interaction with surrounding medium and termination

4.1 Introduction

The best-studied regions of jet termination and the best examples of interactions of jets with the surrounding medium are furnished by radio-loud AGN, The parsec-scale AGN jets discussed in Section 3 generally feed into kpc-scale structures — kpc-scale jets, plumes, lobes and hotspots. The magnetic fields in these structures must exhibit some continuity with the fields set by the jet launching process (Section 2) and exhibited on the parsec scale (Section 3), particularly in the inner parts of kpc-scale jets. However, on the hundred-kpc scales of the jet termination and the downstream structures such as lobes and plumes, it seems likely that much of the initial structure has been erased. As is the case on parsec scales, the intrinsic polarization of synchrotron emission gives us information about the direction and degree of ordering of the magnetic field, though we always need to bear in mind that what we can measure is a projected, polarized-emission-weighted line-of-sight average of the intrinsic degree of polarization and the E- or B-vector angle. In addition, Faraday rotation both external and internal to the emitting medium has an effect on what we observe. A good deal is known about the polarization properties of radio-loud AGN on the largest scales, and we summarize the observational situation in Sections 4.3, 4.4 and 4.5. We then go on to discuss the relationship between observations and modelling in Section 4.6 and the situation in the comparable structures in stellar-scale outflows in Section 4.7. Before that, however, we discuss the methods by which magnetic field strength can be measured in AGN on these scales.

4.2 Measuring magnetic field strengths on the kpc scale

Unfortunately, synchrotron radiation on large scales can tell us little or nothing about the magnetic field *strength*, although this is clearly a key piece of information in understanding the dynamics and energetics of the jet and its environment, without significant (and possibly incorrect) additional assumptions. The methods discussed in Section 3.2 can only be applied in regions with a well-known structure and a non-negligible optical depth, and kpc-scale structures are almost always optically thin at accessible frequencies.

The standard equipartition/minimum energy assumptions (Burbidge 1956) are widely used, but even at best only provide us with a plausible order of magnitude estimate of the magnetic field strength: there is no a priori reason to suppose that the plasma reaches the

minimum energy or equipartition conditions, and even if it does, these assumptions require us to guess the appropriate values for the filling factor and the fraction of energy in non-radiating particles, ϕ and κ in the standard notation for equipartition:

$$\frac{B^2}{2\mu_0} = \frac{1+\kappa}{\phi} \int EN(E)\mathrm{d}E \tag{13}$$

Finally, long-standing practice in the radio-galaxy community is to carry out the integral in eq. (13) over a fixed range in *observed frequency*, not in electron energy, although the latter seems more physically reasonable (Myers and Spangler 1985; Brunetti et al. 1997; Hardcastle et al. 1998) and the differences between these two sets of assumptions can lead to significantly different results (Beck and Krause 2005).

If equipartition and minimum energy are unsatisfactory, what else is available? Another widely used approach that gives at least some constraints is to consider the properties of a medium external to the radio source, which may be easier to measure. For example, thermal bremsstrahlung in the X-ray from the environments of large-scale jets and lobes can give us measurements of the temperature and density, and therefore pressure, of the external environment. On the reasonable assumption that the pressure in a radio-emitting component cannot be much less than that in the medium in which it is embedded, we therefore have a constraint on the total energy density in the source. Combining this with the synchrotron measurements, we can derive values for the magnetic field strength. However, these are not unique (for a given pressure greater than the minimum pressure there are two possible values of B to choose from) and the method is still dependent on assumptions about κ and ϕ as well as field geometry.

By far the best method of measuring magnetic field strength in extended components of radio-loud AGN is the use of inverse-Compton emission. The volume emissivity from the inverse-Compton process depends essentially on the electron and photon number densities as a function of energy. If the properties of the photon field are known, a detection of inverse-Compton emission gives us a constraint on the normalization of the electron energy spectrum. We can use this in combination with a measurement of synchrotron emissivity to estimate the B-field in a very robust way: assuming we know the geometry from radio observations, the only model dependence comes from our assumptions about the shape of the electron energy spectrum, since typically we will be observing energetically different electron populations using the two processes. For very simple spatial and spectral properties of the electron populations, analytical estimates of B from inverse-Compton detections can be derived (e.g. Harris and Grindlay 1979); for more complex situations, numerical codes must be used to integrate the relevant equations (e.g. Hardcastle et al. 1998; Brunetti et al. 2001; Hardcastle et al. 2002).

Inverse-Compton emission from large-scale components of radio-loud AGN was first discovered in the X-ray (Harris et al. 1994; Feigelson et al. 1995) and X-ray observations dominate the current applications of this technique of measuring B. A complication of this is that various other processes, including thermal bremsstrahlung from the hot phase of the IGM and synchrotron emission from high-energy electrons, can produce X-ray emission from the radio sources and their environments. In the following subsections we will discuss the available constraints on magnetic field strengths using this method, bearing in mind these observational limitations.

4.3 Magnetic fields in kpc-scale jets

Kpc-scale jets are often strongly polarized, as discussed in Section 3.8. In the most powerful jets, the apparent magnetic field direction after correction for Faraday rotation is normally along the jet, often following bends in the jet very closely (e.g. Bridle et al. 1994). In the less powerful jets of FRI radio galaxies, there is often a transition between a parallel field configuration in the inner few kpc to a perpendicular field in the centre of the jet further out: parallel fields may be observed at the edge of the jet (e.g. Bridle and Perley 1984). These FRI jets are the jets that have been studied in the greatest detail to date, because their proximity and relative brightness allows sensitive measurements to be made in regions of the jet that are transversely resolved on scales from sub-arcsec to tens of arcsec (hundreds of pc to a few kpc, at typical distances). In addition, both a jet and counterjet are routinely detected in FRIs, and the assumption that the jet and counterjet are intrinsically symmetrical is a viable one, allowing the effects of relativistic beaming and aberration to be separated from the intrinsic (rest-frame) behaviour of the source. Detailed modelling of these FRI jets (e.g. Laing and Bridle 2002; Laing et al. 2006) shows that the observed polarization structures can be modelled in terms of a magnetic field that is locally random but anisotropic. The anisotropic component of the field is mainly a combination of toroidal and longitudinal components, with the toroidal component dominating both at the edges of the jets and at large distances from the nucleus. Globally ordered helical models for the magnetic field (cf. Section 3.5) have been ruled out in some of the best-studied cases (Canvin et al. 2005; Laing et al. 2006): if the field is initially helical, it must evolve away from such a configuration by the kpc scale.

Measurement of B-field strengths in jets is more difficult; although resolved X-ray emission from jets is common (see e.g. Harris and Krawczynski 2006 for a review), there are two fairly serious problems in using them to determine B. The first is that some of the X-ray emission seen from these structures, particularly in low-power objects, is unequivocally known to be synchrotron in origin (e.g. Hardcastle et al. 2001b). Where synchrotron emission is dominant, we only have a (usually uninteresting) lower limit on B in the jet. The second is that the jets of the most powerful objects are known to be at least mildly relativistic on kpc scales (Bridle et al. 1994; Wardle and Aaron 1997; Hardcastle et al. 1999; Mullin and Hardcastle 2009) and this introduces additional model dependence into any estimates of B, since the observed properties of the jet now depend on the bulk Lorentz factor Γ and the angle to the line of sight θ. A good deal of interest was triggered by the discovery that the X-ray emission from the powerful source PKS 0637−752 (Schwartz et al. 2000), which could not be explained by a one-zone synchrotron model, could be explained as inverse-Compton scattering of the CMB with a magnetic field close to equipartition, using a Lorentz factor ($\Gamma \sim 10$) and angle to the line of sight close to those implied by VLBI observations in the nucleus (Tavecchio et al. 2000; Celotti et al. 2001), which would imply no jet deceleration from pc to hundred-kpc scales. However, this certainly does not seem to be the case for all such powerful quasars (Hardcastle 2006) and later work on the broadband SED of the knots in the best-studied example of this class, 3C 273, suggests that the data are inconsistent with an inverse-Compton model anyway (Jester et al. 2002, 2005). As yet there is therefore no likelihood of being able to determine large-scale magnetic fields from inverse-Compton emission in the jets of the most powerful objects, though in (bright, nearby) lower-power objects we may hope for inverse-Compton emission at higher energies (see Section 5.3).

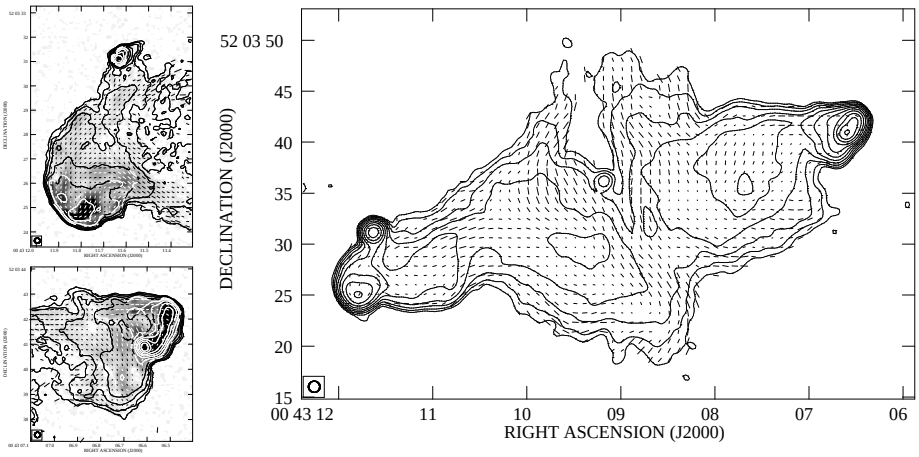

Fig. 8 Complex polarization structure in the lobes and hotspots of the FRII radio galaxy 3C 20 at 8 GHz. Right: the overall structure of the source. Top left: the E hotspot. Bottom right: the W hotspot. Polarization vectors have length representing fractional polarization and are plotted at 90° to the direction of the polarization E-vector, thus giving a representation of the magnetic field direction. Contours show total intensity, increasing logarithmically by a factor of 2 at each step. The greyscales shown for the hotspots indicate polarized intensity to give an idea of the complex filamentary structure that is visible in polarized emission. Data from Hardcastle et al. (1997).

4.4 Jet termination

The bright compact regions at the terminations of powerful jets, known as hotspots, are believed to be shocks at which the jet material interacts with plasma already present in the lobes. They are well studied in the radio because of their high surface brightness, and polarization observations at high resolution (e.g. Carilli et al. 1999) show them to have complex polarization structures (e.g. Fig. 8), presumably because of the complex hydrodynamics in this part of the source. There is a general tendency for the inferred magnetic field angle to be perpendicular to the jet direction on entry to the hotspot (e.g. Leahy et al. 1997; Hardcastle et al. 1997), possibly because of field compression at the shock.

Because the hotspots are often the brightest compact features in sources in which they occur, they would be expected *a priori* to be good sources of so-called synchrotron self-Compton (SSC) emission, where synchrotron emission provides the seed photons for inverse-Compton scattering (Fig. 9). Observational constraints suggest that the bulk flow through hotspots is at best mildly relativistic (e.g. Mullin et al. 2008) and so beaming is less important. Early observations of X-ray emission from hotspots were consistent in many cases with the X-rays being SSC and the magnetic field strengths implied being close to equipartition (Harris et al. 1994, 2000; Hardcastle et al. 2001a, 2002). However, at the same time, a number of hotspots showed X-ray emission that was much brighter than the expectation from SSC at equipartition and (in some cases) was spectrally inconsistent with being SSC at all; this X-ray emission seemed likely to be partly or wholly synchrotron in origin (e.g. Harris et al. 1998; Wilson et al. 2001). Hardcastle et al. (2004), based on the large amount of hotspot data collected in the first few years of the *Chandra* mission, showed that it was plausible that the difference was controlled by the luminosity, and hence the magnetic field strength, of the hotspots (cf. Brunetti et al. 2003); the most luminous hotspots have magnetic field strengths high enough that strong synchrotron losses inhibit the acceleration of elec-

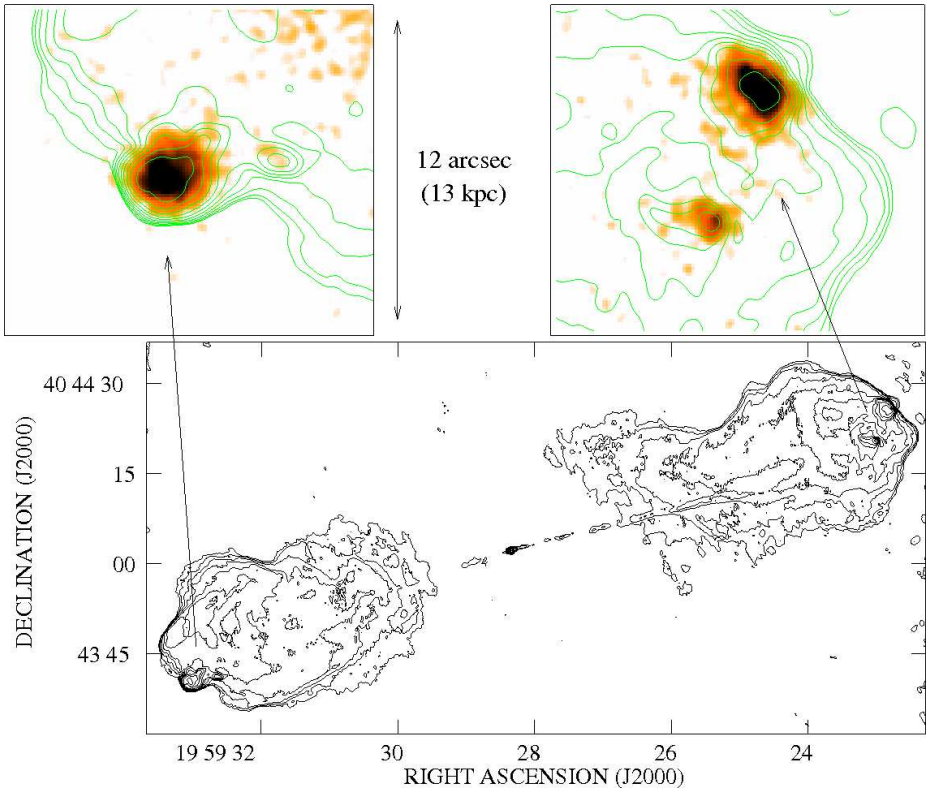

Fig. 9 Synchrotron self-Compton X-ray emission from the hotspots of Cygnus A (3C 405), as first reported by Harris et al. (1994). Lower panel: contours show the 4.5-GHz radio emission from the whole source, from the image of Carilli et al. (1991). Upper panel shows the same contours overlaid on smoothed *Chandra* data in the 0.5-5.0 keV range from the dataset of Wilson et al. (2006). Note the close morphological agreement between radio and X-ray emission. The level of the inverse-Compton emission implies field strengths close to the equipartition value in the hotspots.

trons to energies at which X-ray synchrotron emission would be detected. If this is the case, then it is plausible that all hotspots, not just the subset for which SSC has been detected, have magnetic fields close to the equipartition value (Hardcastle et al. 2004; Kataoka and Stawarz 2005). Remarkably, therefore, it seems that there is a rapidly-acting (since hotspots are short-lived), small-scale physical process that acts to amplify magnetic field strengths up to values within a factor of a few of their equipartition values. These field strengths may be up to 20 nT (200 μG) in the brighest sources.

4.5 Lobes

Beyond the end of the jet and the jet termination shock, if present, are the structures fed by the jet. The most common structure seen is large-scale lobes of synchrotron-emitting material extending back towards the centre of the host galaxy, although extended diffuse plumes are seen in a minority of low-power radio galaxies.

The lobes are often strongly polarized, with the typical apparent magnetic field direction being parallel to contours of constant total intensity surface brightness (e.g. Fig. 8). Because of the large spatial scales, strong polarization and large sizes of magnetic field structures, lobes are the best places for detailed studies of Faraday rotation intrinsic to the source or its local environment. The change in polarization position angle $\Delta\theta$ produced by a foreground Faraday screen is given by $\Delta\theta = RM\,\lambda^2$, where RM is the rotation measure,

$$RM = C \int n_e \, \mathbf{B} \cdot \mathrm{d}\mathbf{l} \tag{14}$$

Thus in principle, with multi-wavelength observations to give the required λ^2 coverage, we can measure both RM and the intrinsic polarization angle and so constrain the electron density and field strength in the Faraday screen. In practice, there are a number of complications (e.g. Laing 1984). Faraday-active material (thermal electrons) *inside* the synchrotron-emitting region will induce depolarization and departures from a λ^2 law; in fact, the absence of this effect gives very strong, albeit model-dependent, limits on the possible densities of thermal electrons inside the lobes (e.g. Dreher et al. 1987). Even if the Faraday screen is external to the lobes, its characteristic size scale must be fully resolved by the radio observations, otherwise beam depolarization results and the problem of determining n_e and B becomes much harder (though in some circumstances it is possible, see e.g. Hardcastle et al. 2010). When Faraday rotation external to the radio galaxy is measured, the derived RM values are consistent with being due to the hot phase of the intracluster medium, and with constraints on the external density the field strengths may be estimated. Observed RM values range from ± 100 rad m^{-2} in typical radio galaxies to ± 4000 rad m^{-2} in Cygnus A, at the centre of a rich cluster (Dreher et al. 1987) and the estimated energy densities in magnetic fields are then comparable to the thermal energy densities of the plasma. The structures observed in Faraday rotation may also be used to constrain the power spectrum of magnetic field fluctuations in the external medium (Laing et al. 2008). However, in the absence of *internal* Faraday rotation, for which there is no conclusive evidence in any object on kpc scales, these estimates of B tell us nothing about the field strength or its variations in the lobes themselves.

The lobes are expected to be particularly good sources of inverse-Compton emission from scattering of diffuse photon populations such as the CMB and the extragalactic background light (Fig. 10). Because their geometry and synchrotron properties are also relatively well constrained, because it is certain that they do not have relativistic bulk motions, and because there is no evidence in general for significant ongoing particle acceleration, they represent the best cases for modelling and hence inverse-Compton observations give the cleanest constraints on magnetic field strengths. Early observations with *ROSAT* and *ASCA* allowed some field measurements to be made (e.g. Feigelson et al. 1995), but again it was *Chandra* and to some extent *XMM-Newton* that gave us comparatively large samples (Hardcastle et al. 2002; Croston et al. 2004, 2005; Kataoka and Stawarz 2005). These provide a very clear picture: both the detections and the non-detections of inverse-Compton emission are consistent with a picture in which the characteristic magnetic field in the lobes is close to, but in general slightly below, the equipartition value. The actual field strength value depends strongly on the lobe size and power, but might be of order 0.1–few nT (1 to a few tens of μG) in large, bright sources, with the energy density in electrons being perhaps an order of magnitude higher. Thus it seems that the mechanism that ensures (approximate) equipartition in the hotspot regions may also operate on the much larger, hundred-kpc scales of the lobes.

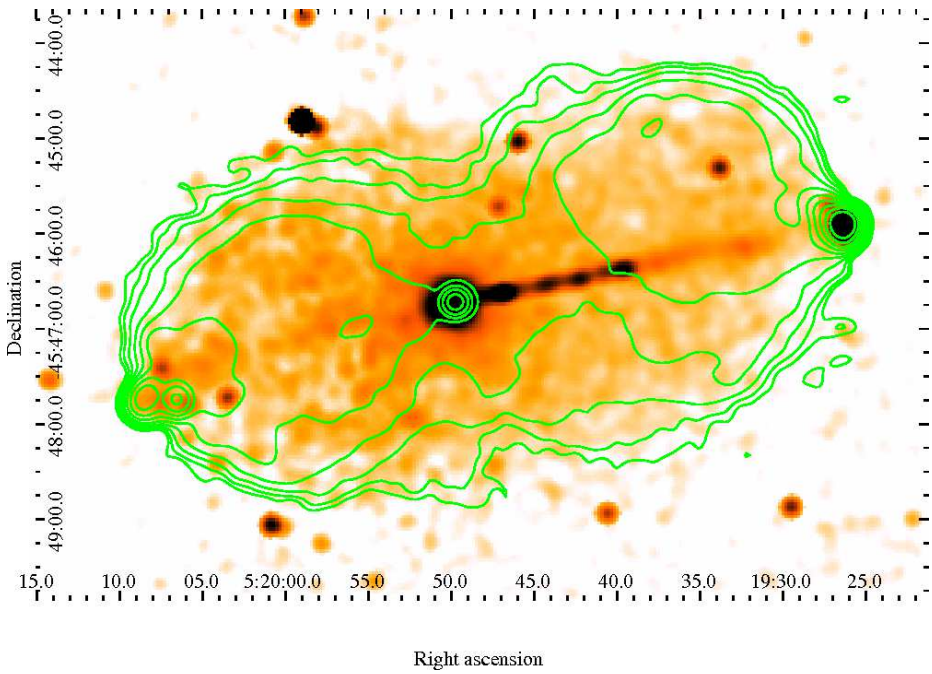

Fig. 10 X-ray emission from the nearby FRII radio galaxy Pictor A. The colour scale shows Gaussian-smoothed *Chandra* counts in the 0.5-5.0 keV range, using the data described by Marshall et al. (2010): contours are from the 1.4-GHz radio map of Perley et al. (1997). Note the X-ray emission (most likely synchrotron, see Hardcastle and Croston 2005) from the jet and hotspot, the excellent match between the boundaries of the X-ray and radio emission, and the relatively constant X-ray surface brightness of the lobes, in contrast to the strongly varying radio surface brightness (contours are logarithmic, increasing by a factor 2 at each step).

We can go slightly further in the best-studied systems, since the fact that the synchrotron and inverse-Compton emission can be *resolved* with *Chandra* and *XMM-Newton* means that we are not restricted to considering one-zone models, as first realised by Isobe et al. (2002). Hardcastle and Croston (2005) showed that in fact the magnetic field strength has to vary by a factor of up to 2 throughout the lobe of the best-studied lobe IC source, Pictor A (Fig. 10), in the sense that the field strength decreases with distance from the hotspot. More recently, Goodger *et al.* (in prep.) have used inverse-Compton data to argue that the strongly filamentary structure seen in synchrotron observations of many powerful radio sources must be a result of strong small-scale variations of the magnetic field strength (if it were the electron energy density that was varying, there would be a stronger correlation between the synchrotron and inverse-Compton emission than is observed). Although this detailed work is at the limits of what is presently achievable with X-ray observations, it may be the only way in which the detailed relationship between field and electrons in the lobes can be studied.

The limitation of the lobe inverse-Compton technique is that it can only really be used to study sources in which the diffuse X-ray emission is not dominated by thermal bremsstrahlung from the IGM; i.e. objects in relatively poor environments. Among other things, this means that with the exception of Cen A (see below, Section 5.3) there is no inverse-Compton estimate of the magnetic field strength in the lobes of any low-power (FRI) source,

although inverse-Compton limits have been used to constrain the particle content in such objects (e.g. Jetha et al. 2008; Hardcastle and Croston 2010).

4.6 Modelling of large-scale fields

Analytical modelling of the dynamics of the lobes of radio galaxies has since its beginning focussed on a pure hydrodynamical approach (e.g. Scheuer 1974; Kaiser and Alexander 1997) and numerical modelling has often followed suit (e.g. Basson and Alexander 2003; Krause 2005). To some extent, this approach may be (retrospectively) justifiable by the inverse-Compton observations discussed above (Section 4.5), which tell us that magnetic fields cannot dominate the large-scale dynamics. Nevertheless, numerical modelling involving magnetic fields is important for three reasons; firstly, even synthetic synchrotron mapping requires some idea of the magnetic field strength distribution, while reproducing observations of polarization and RM/depolarization structures (see above) is impossible without a model of the magnetic field both in the radio source and the environment; secondly, while the magnetic field may not dominate the dynamics of the large-scale structures, it may still have a dynamical role to play, for example in suppressing Kelvin-Helmholtz instabilities; and thirdly, such modelling in principle allows us to test assumptions about the transport of the magnetic field structures imposed at jet generation and observed in the parsec-scale jet (Sections 2 and 3).

The earliest simulations of lobe dynamics involving magnetic field structure (Clarke et al. 1989; Matthews and Scheuer 1990) involved passive transport of the field, but more recently it has been possible to numerically solve the full MHD equations for semi-realistic density, jet speed and magnetization regimes. Some compromises have generally been necessary to allow such simulations. For example, the work of Jones et al. (1999), Tregillis et al. (2001) and Tregillis et al. (2004) considered electron transport and radiative losses, but operated in a uniform environment. MHD simulations involving realistic large-scale atmospheres, matched to the information derived from X-ray observations (e.g. O'Neill et al. 2005; Gaibler et al. 2009; O'Neill and Jones 2010) tend to neglect electron radiative losses and also, in earlier work, tend to consider rather low jet density contrasts. Increased computational power has started to allow the merger of these two approaches (e.g Mendygral et al. 2012). Key results from this modelling to date include the broad reproduction of the lobe dynamics expected from hydrodynamical analytic or numerical modelling; the suppression of large-scale Kelvin-Helmholtz instabilities and of the entrainment of external gas seen in pure hydrodynamic modelling (Gaibler et al. 2009), and the emergence of complex small-scale structure in the magnetic field and hence the synchrotron emissivity (e.g. Tregillis et al. 2001). 3D MHD simulations which can simultaneously capture realistic large-scale dynamics and have resolution good enough to be matched to the detailed observations of synchrotron and inverse-Compton emission in radio galaxy lobes, so as to help with questions such as the origin of filamentary structures seen in synchrotron emission (Section 4.5) can perhaps be expected in the next few years. Numerical modelling is also perhaps starting to shed some light on the *origins* of the field structures on large scales; for example, Gaibler et al. (2009) put in as an input condition a helical field as observed in parsec-scale AGN jets (Section 3), and show that this initial field is amplified by shear processes to reach much larger values than expected from flux conservation. On the other hand, Huarte-Espinosa et al. (2011) are able to reproduce many features of real radio galaxy lobes with a field which is initially *random* (in both the jet and the environment into which it propagates). It will be of great interest to see whether high-resolution simulations of large-

scale jet-environment interactions can give predictions which would allow us to distinguish between different models of the small-scale jet magnetic field structure.

4.7 Large-scale magnetic fields in stellar-scale outflows

The study of the terminations and the equivalents of lobes in stellar-scale outflows such as protostellar jets and microquasars is much less well developed. These structures require persistent jets, and so impulsive ejection events such as those seen in some microquasars are not expected to produce them. Where jets are persistent or at least recurrent on short timescales,, there is evidence in a few well-studied microquasars for lobe-like synchrotron emission (e.g Mirabel et al. 1992; Fabrika 2004; Hardcastle 2005) and even both lobes and hotspots (Soria et al. 2010), as well as indirect evidence for the existence of lobes whose synchrotron emission is not seen in some other cases (Gallo et al. 2005). The lack of lobes in general in these systems has been attributed to the low-density environments in which they reside (Heinz 2002). Even when found, though, these lobes are generally faint, so that even polarization measurements are generally not possible, and techniques such as magnetic field strength measurements by inverse-Compton emission are completely out of the question, even setting aside the complex technical challenges of doing so in the presence of an often strong central X-ray source and of a complex and poorly constrained photon field. Authors wishing to estimate magnetic field strengths use the equipartition assumption, despite its limitations (Section 4.2).

Turning to protostellar outflows, models for these systems fall into two general categories: a jet-driven bow shock picture analoguous to the dynamics of FRII radio galaxies, and a wind-driven shell picture in which the molecular gas is driven by an underlying wide-angle wind component, such as is given by the X-wind (Cabrit et al. 1997). A survey of molecular outflows by Lee et al. (2000) found that both mechanisms are needed in order to explain the full set of systems observed. The advent of Spitzer observations of protostellar jets has led to spectacular advances in our understanding of jet morphology, shock structure, and jet termination. For example, the jet in the classic T-Tauri star system HH46/47, imaged in the infrared with high resolution techniques (down to sub-arcsec levels), is bright and highly collimated and has both a wide-angle outflow cavity as well as a collimated jet that extends through all scales from the protostellar scale up to the termination point on the bow shock (Velusamy et al. 2007), showing a morphology which is remarkably similar to those of powerful radio galaxies. The jet is well collimated with a width of 1-1.5$''$ and length of 10$''$ (4500 AU). One of the most prominent features are bright “hotspots’; that are coincident with the head of the jet and appear to be analoguous to the hotspots of radio galaxies. Cool molecular gas is detected in the wide-angle flow that surrounds this jet. Similarly, observations of the jet Cep E associated with a more massive forming star (with up to 4 $M_{\odot}$), using the same techniques, show shocked molecular hydrogen H_2 emission — which requires the existence of a magnetic precusor (C-shocks) in order to be excited (Velusamy et al. 2011). Here again, the hottest emission comes from atomic/ionic gas produced at the hot spot at the bow shock of the jet. However, despite this important evidence for magnetization of the shocked region, and unlike the AGN case, there is as yet little direct evidence for the role of magnetic fields in the production of “hotspots” and lobes, since there are few observational diagnostics of field strength in this regime and synchrotron radiation is seldom observed. In the case of protostellar jets, the state of the art, as discussed above (Carrasco-González et al. 2010) is the detection of radio polarization, confirming a synchrotron origin for some of the detected radio continuum, but this is a detection of the jet, rather than of a lobe-like struc-

ture, and here again equipartition assumptions must be used to estimate a magnetic field strength. Next-generation radio and X-ray facilities will be required for the study of these systems to catch up with that of extragalactic large-scale lobes.

5 New directions

5.1 Magnetic field strengths and directions in protostellar jets

The Expanded VLA (EVLA) and the extended Multi-Element Radio Linked Interferometer (e-MERLIN) will have an order of magnitude more sensitivity than their predecessors. Much larger parts of the radio spectrum will be measured as a consequence, and this will have a huge impact on our ability to measure synchrotron radiation from protostellar systems. The one detected source HH80-81 is one of the most powerful TTS jets known. If the weaker jets turn out to have measurable synchrotron emission, this will herald a new era in the study of jets in general, and of their magnetic field structure in particular.

A second major advance in understanding the launch of jets will come with the ALMA observatory. ALMA observations will allow one to resolve the 1-AU scale of nearby protostellar discs for the first time. The important point is that ALMA will also be able to measure linearly polarized emission. It is expected that this will allow one to map the structure of magnetic fields on the disc, and, in this way, to study the structure of the disc field and its connection to the launch mechanism.

The bottom line is that the era of real magnetic field measurements in protostellar systems is very near — and this will help revolutionize our knowledge of how jets are launched and collimated.

5.2 Parsec-scale magnetic fields in AGN: Physics of the launching, propagation and confinement of the jets

Observations with the Very Long Baseline Array over the past decade have made the importance of high-resolution, multi-frequency, polarization-sensitive radio studies with VLBI abundantly clear. The availability of spectral information can help identify locations of particle re-acceleration and low-frequency absorption in the jets, and the Faraday rotation distribution can provide information about both the thermal gas in the vicinity of the AGN and the intrinsic magnetic fields of the jets themselves. The question of whether there is an appreciable helical or toroidal component is of crucial importance for our understanding of the launching and confinement of the jets, and will be a key aspect of future observational studies. Multi-frequency polarization VLBI observations of more AGNs are very much needed for these reasons.

Faraday-rotation studies on parsec scales with high resolution are of particular interest; however, work of this kind has been hindered by the fact that increasing resolution requires observing at higher frequencies, whereas increasing the sensitivity to Faraday rotation requires observing at lower frequencies. One promising way to overcome this limitation is through space VLBI observations at centimetre wavelengths. The currently flying RadioAstron mission is likely to be of only limited use for this purpose, since it has limited imaging capability due to the elongated orbit of the space antenna. The Japanese-led VSOP2 mission would have provided much better imaging capability, but, unfortunately, this mission has recently been cancelled. It will be important to ensure that any other future space-VLBI

missions include frequencies low enough (8, 5 and possibly even 1.6 GHz) to make these power tools for high-resolution Faraday-rotation studies. On the other hand, polarization observations at 3 mm-1.3 cm sampling subparsec scales could also prove valuable for future Faraday-rotation studies, since these will probe regions with high electron densities and high magnetic fields in the innermost jets, where very high Faraday rotations may be reached.

Another area in which future VLBI observations can play an important role is in relatively low-frequency multi-frequency observations with global arrays such as the VLBA. Such observations can help link up the parsec scales studied this far with VLBI and the kpc scales that will be studied with high sensitivity using the EVLA and e-MERLIN. One such project is a recently completed set of four-wavelength 18-22 cm polarization VLBA observations of the 135 AGNs in the main MOJAVE sample, which typically provide information about the jet structures out to scales of tens of parsec. Observations of additional AGNs at these and longer wavelengths would be of considerable interest. It is thus extremely important to develop techniques for accurate intensity, polarization and polarization position angle calibration of such long-wavelength VLBI data.

5.3 Kiloparsec-scale AGN: new approaches to field direction and strength

The EVLA, and other next-generation radio telescopes with observing bandwidths of order GHz rather than tens of MHz, will have a great impact on the study of Faraday rotation in the large-scale polarized components of radio galaxies. Rather than requiring many monochromatic multi-frequency observations, it will in many cases be possible to make a good measurement of RM and depolarization with a single broad-band observation. This should allow the results obtained from detailed studies of bright objects in rich environments (Dreher et al. 1987; Perley and Carilli 1996) to be generalized to more typical systems. The sensitivity and resolution provided by the EVLA and e-MERLIN will allow the detailed, quantitative study of polarization structures in jets (Section 4.3) to be extended to more objects, to smaller scales (connecting 100-pc and pc-scale jets) and possibly to the large-scale jets in FRII sources. At lower frequencies, instruments such as LOFAR with the capability to measure polarization sensitively at low frequencies may allow us to probe the RM due to very tenuous, large-scale gas seen in front of the polarized outer regions of giant radio galaxies, giving constraints on n_e and B on these scales that are currently unobtainable in any other way.

Progress in inverse-Compton measurements of B will also have to come from new observational developments. Currently one problem with the method is the extrapolation between the properties of the $\gamma \approx 1000$ electrons responsible for inverse-Compton scattering CMB photons into the X-ray band and the $\gamma \approx 10^4$ electrons responsible for radio synchrotron emission at GHz frequencies. This situation will be improved significantly with the advent of next-generation low-frequency radio telescopes such as LOFAR. We can also hope, with less certainty, for imaging missions working at harder X-ray energies, such as NuSTAR, which will not only probe somewhat higher-energy electrons but, by operating above the cutoff energies for thermal bremsstrahlung, will make it much easier to study inverse-Compton emission from sources in rich environments. Another ambiguity in models is the correct modelling of the very low-energy electron population: as shown by Colafrancesco (2008), ALMA may in principle be able to detect the Sunyaev-Zel'dovich effect from radio galaxy lobes, which is a very strong probe of the total number of relativistic electrons and hence of the low-energy cutoff (although see Hardcastle and Looney 2008 for some caveats). Finally, inverse-Compton studies at very high energies have some promise. *Fermi* recently

made the first detection of what appears to be inverse-Compton scattering of the CMB to $\sim$ GeV energies, in the nearby, and therefore very large in angular size, radio galaxy Cen A (Abdo et al. 2010): taken at face value the detection implies a magnetic field strength in the lobes that is again close to the equipartition value. *Fermi* can resolve only a very few nearby and (necessarily) atypical radio galaxies, but even limits from this process may be useful. At higher energies still, existing detections with TeV imaging instruments such as HESS and MAGIC place limits on inverse-Compton scattering (predominantly of starlight: Stawarz et al. 2003) by the TeV electrons in the jets of low-power radio galaxies: for example, existing HESS detections of Cen A, whose synchrotron properties are very well known (e.g. Hardcastle et al. 2007 and refs therein) already require that the magnetic field cannot be too much lower than the equipartition value, although detailed modelling is complex (Hardcastle and Croston 2011). The resolution and sensitivity that will be achieved with instruments such as the planned Cerenkov Telescope Array (CTA) will actually allow imaging of the TeV inverse-Compton jets in objects such as Cen A, if $B \approx B_{\rm eq}$, and so will permit mapping of the B-field in an X-ray synchrotron jet for the first time. In the very long term, X-ray telescopes with very high sensitivity (e.g., the currently planned *Athena* mission) may allow us to measure inverse-Compton emission from the lobes of Galactic microquasars and synchrotron-emitting protostellar jets (Section 4.7).

6 Conclusion

In conclusion, this review has covered a vast amount of observational, theoretical and computational phase space with the purpose of drawing out and analyzing the importance of magnetic fields for the origin and structure of astrophysical jets. The underlying engines for all of these systems involves rotating magnetized objects such as stars, black holes, and accretion discs. Relativistic and even general relativistic MHD leads to similar conclusions about jet dynamics to those deduced (and in some cases observed) in protostellar systems. While measurements of densities, temperatures, and velocities is straightforward in the latter type of system, magnetic measurements are very difficult. Exactly the opposite is the case for AGN jets. Encompassing these two complementary worlds lies the complete picture of astrophysical jets which is still in a very exciting stage of exploration. It will be important therefore to keep probing and extending our ability to measure magnetic field strengths and geometries in these diverse systems, since these provide insight into the origin of one nature's most marvellous creations.

Acknowledgements

We thank André Balogh and the organizers of an ISSI workshop on "Large Scale Magnetic Fields in the Universe" for their invitation to review this topic. This paper has benefited from helpful comments from an anonymous referee. The research of REP is supported by a Discovery Grant from the National Science and Engineering Research Council of Canada. MJH acknowledges support from the Royal Society and the UK Science and Technology Funding Council.

References

A.A. Abdo, M. Ackermann, M. Ajello, W.B. Atwood, L. Baldini, J. Ballet, G. Barbiellini, D. Bastieri, B.M. Baughman, K. Bechtol, R. Bellazzini, B. Berenji, R.D. Blandford, E.D. Bloom, E. Bonamente, A.W. Borgland, J. Bregeon, A. Brez, M. Brigida, P. Bruel, T.H. Burnett, S. Buson, G.A. Caliandro, R.A. Cameron, P.A. Caraveo, J.M. Casandjian, E. Cavazzuti, C. Cecchi, Ö. Çelik, A. Chekhtman, C.C. Cheung, J. Chiang, S. Ciprini, R. Claus, J. Cohen-Tanugi, S. Colafrancesco, L.R. Cominsky, J. Conrad, L. Costamante, S. Cutini, D.S. Davis, C.D. Dermer, A. de Angelis, F. de Palma, S.W. Digel, E. do Couto e Silva, P.S. Drell, R. Dubois, D. Dumora, C. Farnier, C. Favuzzi, S.J. Fegan, J. Finke, W.B. Focke, P. Fortin, Y. Fukazawa, S. Funk, P. Fusco, F. Gargano, D. Gasparrini, N. Gehrels, M. Georganopoulos, S. Germani, B. Giebels, N. Giglietto, F. Giordano, M. Giroletti, T. Glanzman, G. Godfrey, I.A. Grenier, J.E. Grove, L. Guillemot, S. Guiriec, Y. Hanabata, A.K. Harding, M. Hayashida, E. Hays, R.E. Hughes, M.S. Jackson, Jóhannesson G., S.Johnson, T.J.Johnson, W.N.Johnson, T.Kamae, H.Katagiri, J.Kataoka, N.Kawai, M.Kerr, J.Knödlseder, M.L.Kocian, M.Kuss, J.Lande, L.Latronico, M.Lemoine-Goumard, F.Longo, F.Loparco, B.Lott, M.N.Lovellette, P.Lubrano, G.M.Madejski, A.Makeev, M.N.Mazziotta, W.McConville, J.E.McEnery, C.Meurer, P.F.Michelson, W.Mitthumsiri, T.Mizuno, A.A.Moiseev, C.Monte, M.E.Monzani, A.Morselli, I.V.Moskalenko, S.Murgia, P.L.Nolan, J.P.Norris, E.Nuss, T.Ohsugi, N.Omodei, E.Orlando, J.F.Ormes, D.Paneque, D.Parent, V.Pelassa, M.Pepe, M.Pesce-Rollins, F.Piron, T.A.Porter, S.Rainò, R.Rando, M.Razzano, S.Razzaque, A.Reimer, O.Reimer, T.Reposeur, S.Ritz, L.S.Rochester, A.Y.Rodriguez, R.W.Romani, M.Roth, F.Ryde, H.F.W.Sadrozinski, R.Sambruna, D.Sanchez, A.Sander, P.M.Saz Parkinson, J.D.Scargle, C.Sgrò, J.Siskind, D.A.Smith, P.D.Smith, G.Spandre, P.Spinelli, J.L.Starck, L.Stawarz, M.S.Strickman, D.J.Suson, H.Tajima, H.Takahashi, T.Takahashi, T.Tanaka, J.B.Thayer, J.G.Thayer, D.J.Thompson, L.Tibaldo, D.F.Torres, G.Tosti, A.Tramacere, Y.U.Uchiyama T. L., V.Vasileiou, N.Vilchez, V.Vitale, A.P.Waite, E.Wallace, P.Wang, B.L.Winer, K.S.Wood, T.Ylinen, M.Ziegler, M.J.Hardcastle, D.Kazanas, Fermi-LAT Collaboration, Fermi Gamma-Ray Imaging of a Radio Galaxy. Science **328**, 725 (2010). doi:10.1126/science.1184656

J.M. Anderson, Z.Y. Li, R. Krasnopolsky, R.D. Blandford, Locating the Launching Region of T Tauri Winds: The Case of DG Tauri. Astrophys. J. Lett. **590**, 107–110 (2003). doi:10.1086/376824

K. Asada, M. Inoue, Y. Uchida, S. Kameno, K. Fujisawa, S. Iguchi, M. Mutoh, A Helical Magnetic Field in the Jet of 3C 273. Proc. Astron. Soc. Jpn. **54**, 39–43 (2002)

K. Asada, M. Inoue, M. Nakamura, S. Kameno, H. Nagai, Multifrequency Polarimetry of the NRAO 140 Jet: Possible Detection of a Helical Magnetic Field and Constraints on Its Pitch Angle. Astrophys. J. **682**, 798–802 (2008a). doi:10.1086/588573

K. Asada, M. Inoue, S. Kameno, H. Nagai, Time Variation of the Rotation Measure Gradient in the 3C 273 Jet. Astrophys. J. **675**, 79–82 (2008b). doi:10.1086/524000

K. Asada, M. Nakamura, M. Inoue, S. Kameno, H. Nagai, Multi-frequency Polarimetry toward S5 0836+710: A Possible Spine-Sheath Structure for the Jet. Astrophys. J. **720**, 41–45 (2010). doi:10.1088/0004-637X/720/1/41

J.M. Attridge, D.H. Roberts, J.F.C. Wardle, Radio Jet-Ambient Medium Interactions on Parsec Scales in the Blazar 1055+018. Astrophys. J. Lett. **518**, 87–90 (1999). doi:10.1086/312078

F. Bacciotti, T.P. Ray, R. Mundt, J. Eislöffel, J. Solf, Hubble Space Telescope/STIS Spectroscopy of the Optical Outflow from DG Tauri: Indications for Rotation in the Initial Jet Channel. Astrophys. J. **576**, 222–231 (2002). doi:10.1086/341725

F. Bacciotti, T.P. Ray, D. Coffey, J. Eislöffel, J. Woitas, Testing the Models for Jet Generation with Hubble Space Telescope Observations. Astrophys. Space Sci. **292**, 651–658 (2004). doi:10.1023/B:ASTR.0000045071.52869.a4

J. Bally, B. Reipurth, C.J. Davis, Observations of Jets and Outflows from Young Stars, in *Protostars and Planets V*, ed. by B. Reipurth, D. Jewitt, K. Keil, 2007, pp. 215–230

R. Banerjee, R.E. Pudritz, Outflows and Jets from Collapsing Magnetized Cloud Cores. Astrophys. J. **641**, 949–960 (2006). doi:10.1086/500496

J.F. Basson, P. Alexander, The long-term effect of radio sources on the intracluster medium. Mon. Not. Roy. Astron. Soc. **339**, 353–359 (2003). doi:10.1046/j.1365-8711.2003.06069.x

R. Beck, M. Krause, Revised equipartition and minimum energy formula for magnetic field strength estimates from radio synchrotron observations. Astronomische Nachrichten **326**, 414–427 (2005). doi:10.1002/asna.200510366

M.C. Begelman, Z.Y. Li, Asymptotic domination of cold relativistic MHD winds by kinetic energy flux. Astrophys. J. **426**, 269–278 (1994). doi:10.1086/174061

N. Bessolaz, C. Zanni, J. Ferreira, R. Keppens, J. Bouvier, Accretion funnels onto weakly magnetized young stars. Astron. Astrophys. **478**, 155–162 (2008). doi:10.1051/0004-6361:20078328

G.S. Bisnovatyi-Kogan, Dynamic confinement of jets by magnetotorsional oscillations. Mon. Not. Roy. As-

tron. Soc. **376**, 457–464 (2007). doi:10.1111/j.1365-2966.2007.11452.x
R. Blandford, Acceleration and collimation mechanisms in jets., in *Astrophysics and Space Science Library*. Astrophysics and Space Science Library, vol. 103, 1993, pp. 15–33
R.D. Blandford, Black Holes and Relativistic Jets. Progress of Theoretical Physics Supplement **143**, 182–201 (2001). doi:10.1143/PTPS.143.182
R.D. Blandford, A. Konigl, Relativistic jets as compact radio sources. Astrophys. J. **232**, 34–48 (1979). doi:10.1086/157262
R.D. Blandford, D.G. Payne, Hydromagnetic flows from accretion discs and the production of radio jets. Mon. Not. Roy. Astron. Soc. **199**, 883–903 (1982)
R.D. Blandford, R.L. Znajek, Electromagnetic extraction of energy from Kerr black holes. Mon. Not. Roy. Astron. Soc. **179**, 433–456 (1977)
A.H. Bridle, R.A. Perley, Extragalactic Radio Jets. Ann. Rev. Astron. Astrophys. **22**, 319–358 (1984). doi:10.1146/annurev.aa.22.090184.001535
A.H. Bridle, D.H. Hough, C.J. Lonsdale, J.O. Burns, R.A. Laing, Deep VLA imaging of twelve extended 3CR quasars. Astron. J. **108**, 766–820 (1994). doi:10.1086/117112
S. Britzen, R.C. Vermeulen, R.M. Campbell, G.B. Taylor, T.J. Pearson, A.C.S. Readhead, W. Xu, I.W. Browne, D.R. Henstock, P. Wilkinson, A multi-epoch VLBI survey of the kinematics of CFJ sources. II. Analysis of the kinematics. Astron. Astrophys. **484**, 119–142 (2008). doi:10.1051/0004-6361:20077717
A.E. Broderick, J.C. McKinney, Parsec-scale Faraday Rotation Measures from General Relativistic Magnetohydrodynamic Simulations of Active Galactic Nucleus Jets. Astrophys. J. **725**, 750–773 (2010). doi:10.1088/0004-637X/725/1/750
G. Brunetti, G. Setti, A. Comastri, Inverse Compton X-rays from strong FRII radio-galaxies. Astron. Astrophys. **325**, 898–910 (1997)
G. Brunetti, M. Cappi, G. Setti, L. Feretti, D.E. Harris, Anisotropic inverse Compton scattering in powerful radio galaxies: The case of 3C 295. Astron. Astrophys. **372**, 755–767 (2001). doi:10.1051/0004-6361:20010484
G. Brunetti, K.H. Mack, M.A. Prieto, S. Varano, In-situ particle acceleration in extragalactic radio hot spots: observations meet expectations. Mon. Not. Roy. Astron. Soc. **345**, 40–44 (2003). doi:10.1046/j.1365-8711.2003.07185.x
G.R. Burbidge, On Synchrotron Radiation from Messier 87. Astrophys. J. **124**, 416 (1956). doi:10.1086/146237
S. Cabrit, A. Raga, F. Gueth, Models of Bipolar Molecular Outflows, in *Herbig-Haro Flows and the Birth of Stars*, ed. by B. Reipurth & C. Bertout. IAU Symposium, vol. 182, 1997, pp. 163–180
M. Camenzind, Hydromagnetic flows from rapidly rotating compact objects. I - Cold relativistic flows from rapid rotators. Astron. Astrophys. **162**, 32–44 (1986)
J.R. Canvin, R.A. Laing, A.H. Bridle, W.D. Cotton, A relativistic model of the radio jets in NGC 315. Mon. Not. Roy. Astron. Soc. **363**, 1223–1240 (2005). doi:10.1111/j.1365-2966.2005.09537.x
C.L. Carilli, R.A. Perley, J.W. Dreher, J.P. Leahy, Multifrequency radio observations of Cygnus A - Spectral aging in powerful radio galaxies. Astrophys. J. **383**, 554–573 (1991). doi:10.1086/170813
C.L. Carilli, J.D. Kurk, P.P. van der Werf, R.A. Perley, G.K. Miley, High-Resolution Millimeter and Infrared Observations of the Hot Spots of Cygnus A. Astron. J. **118**, 2581–2591 (1999). doi:10.1086/301137
C. Carrasco-González, L.F. Rodríguez, G. Anglada, J. Martí, J.M. Torrelles, M. Osorio, A Magnetized Jet from a Massive Protostar. Science **330**, 1209 (2010). doi:10.1126/science.1195589
F. Casse, R. Keppens, Magnetized Accretion-Ejection Structures: 2.5-dimensional Magnetohydrodynamic Simulations of Continuous Ideal Jet Launching from Resistive Accretion Disks. Astrophys. J. **581**, 988–1001 (2002). doi:10.1086/344340
T.V. Cawthorne, J.F.C. Wardle, D.H. Roberts, D.C. Gabuzda, L.F. Brown, Milliarcsecond Polarization Structure of 24 Objects from the Pearson-Readhead Sample of Bright Extragalactic Radio Sources. I. The Images. Astrophys. J. **416**, 496 (1993). doi:10.1086/173253
A. Celotti, G. Ghisellini, M. Chiaberge, Large-scale jets in active galactic nuclei: multiwavelength mapping. Mon. Not. Roy. Astron. Soc. **321**, 1–5 (2001). doi:10.1046/j.1365-8711.2001.04160.x
T. Chiueh, Z.Y. Li, M.C. Begelman, Asymptotic structure of hydromagnetically driven relativistic winds. Astrophys. J. **377**, 462–466 (1991). doi:10.1086/170375
D. Christodoulou, D. Gabuzda, I. Contopoulos, D. Kazanas, 2012 Transverse Faraday Rotation Measure Gradients Across the Kiloparsec-scale Radio Structures of Active Galactic Nuclei. Submitted to A&A.
D.A. Clarke, J.O. Burns, M.L. Norman, Numerical observations of a simulated jet with a passive helical magnetic field. Astrophys. J. **342**, 700–717 (1989). doi:10.1086/167631
E. Clausen-Brown, M. Lyutikov, P. Kharb, Signatures of large-scale magnetic fields in active galactic nuclei jets: transverse asymmetries. Mon. Not. Roy. Astron. Soc. **415**, 2081–2092 (2011). doi:10.1111/j.1365-2966.2011.18757.x

D. Coffey, F. Bacciotti, L. Podio, T Tauri Jet Physics Resolved Near the Launching Region with the Hubble Space Telescope. Astrophys. J. **689**, 1112–1126 (2008). doi:10.1086/592343

D. Coffey, F. Bacciotti, J. Woitas, T.P. Ray, J. Eislöffel, Rotation of Jets from Young Stars: New Clues from the Hubble Space Telescope Imaging Spectrograph. Astrophys. J. **604**, 758–765 (2004). doi:10.1086/382019

S. Colafrancesco, SZ effect from radio-galaxy lobes: astrophysical and cosmological relevance. Mon. Not. Roy. Astron. Soc. **385**, 2041–2048 (2008). doi:10.1111/j.1365-2966.2008.12961.x

C. Combet, J. Ferreira, The radial structure of protostellar accretion disks: influence of jets. Astron. Astrophys. **479**, 481–491 (2008). doi:10.1051/0004-6361:20078734

I. Contopoulos, D.M. Christodoulou, D. Kazanas, D.C. Gabuzda, The Invariant Twist of Magnetic Fields in the Relativistic Jets of Active Galactic Nuclei. Astrophys. J. Lett. **702**, 148–152 (2009). doi:10.1088/0004-637X/702/2/L148

J. Contopoulos, A Simple Type of Magnetically Driven Jets: an Astrophysical Plasma Gun. Astrophys. J. **450**, 616 (1995). doi:10.1086/176170

J. Contopoulos, R.V.E. Lovelace, Magnetically driven jets and winds: Exact solutions. Astrophys. J. **429**, 139–152 (1994). doi:10.1086/174307

C. Coughlan, R. Murphy, K. McEnery, H. Patrick, R. Hallahan, D. Gabuzda, First results from 18-22cm VLBA polarisation observations of the MOJAVE-I AGNs, in *"Proceedings of the 10th European VLBI Network Symposium and EVN Users Meeting: VLBI and the new generation of radio arrays. September 20-24, 2010. Manchester, UK. Published online at http://pos.sissa.it/cgi-bin/reader/conf.cgi?confid=125, id.46"*, 2010

S.R. Cranmer, Turbulence-driven Polar Winds from T Tauri Stars Energized by Magnetospheric Accretion. Astrophys. J. **689**, 316–334 (2008). doi:10.1086/592566

S.M. Croke, S.P. O'Sullivan, D.C. Gabuzda, The parsec-scale distributions of intensity, linear polarization and Faraday rotation in the core and jet of Mrk501 at 8.4-1.6 GHz. Mon. Not. Roy. Astron. Soc. **402**, 259–270 (2010). doi:10.1111/j.1365-2966.2009.15923.x

J.H. Croston, M. Birkinshaw, M.J. Hardcastle, D.M. Worrall, X-ray emission from the nuclei, lobes and hot-gas environments of two FR II radio galaxies. Mon. Not. Roy. Astron. Soc. **353**, 879–889 (2004). doi:10.1111/j.1365-2966.2004.08118.x

J.H. Croston, M.J. Hardcastle, D.E. Harris, E. Belsole, M. Birkinshaw, D.M. Worrall, An X-Ray Study of Magnetic Field Strengths and Particle Content in the Lobes of FR II Radio Sources. Astrophys. J. **626**, 733–747 (2005). doi:10.1086/430170

B. Davies, S.L. Lumsden, M.G. Hoare, R.D. Oudmaijer, W.J. de Wit, The circumstellar disc, envelope and bipolar outflow of the massive young stellar object W33A. Mon. Not. Roy. Astron. Soc. **402**, 1504–1515 (2010). doi:10.1111/j.1365-2966.2009.16077.x

J.W. Dreher, C.L. Carilli, R.A. Perley, The Faraday rotation of Cygnus A - Magnetic fields in cluster gas. Astrophys. J. **316**, 611–625 (1987). doi:10.1086/165229

D.F. Duffin, R.E. Pudritz, The Early History of Protostellar Disks, Outflows, and Binary Stars. Astrophys. J. Lett. **706**, 46–51 (2009). doi:10.1088/0004-637X/706/1/L46

G.C. Duncan, P.A. Hughes, Simulations of relativistic extragalactic jets. Astrophys. J. Lett. **436**, 119 (1994). doi:10.1086/187647

R.J.H. Dunn, A.C. Fabian, Investigating AGN heating in a sample of nearby clusters. Mon. Not. Roy. Astron. Soc. **373**, 959–971 (2006). doi:10.1111/j.1365-2966.2006.11080.x

S. Fabrika, The jets and supercritical accretion disk in SS433. Astrophysics and Space Physics Reviews **12**, 1–152 (2004)

E.D. Feigelson, S.A. Laurent-Muehleisen, R.I. Kollgaard, E.B. Fomalont, Discovery of Inverse-Compton X-Rays in Radio Lobes. Astrophys. J. Lett. **449**, 149 (1995). doi:10.1086/309642

C. Fendt, Collimation of Astrophysical Jets: The Role of the Accretion Disk Magnetic Field Distribution. Astrophys. J. **651**, 272–287 (2006). doi:10.1086/507976

C. Fendt, Formation of Protostellar Jets as Two-Component Outflows from Star-Disk Magnetospheres. Astrophys. J. **692**, 346–363 (2009). doi:10.1088/0004-637X/692/1/346

C. Fendt, M. Camenzind, On collimated stellar jet magnetospheres. II. Dynamical structure of collimating wind flows. Astron. Astrophys. **313**, 591–604 (1996)

J. Ferreira, Magnetically-driven jets from Keplerian accretion discs. Astron. Astrophys. **319**, 340–359 (1997)

J. Ferreira, Theory of magnetized accretion discs driving jets, in *EAS Publications Series*, ed. by J. Bouvier & J.-P. Zahn. EAS Publications Series, vol. 3, 2002, pp. 229–277

J. Ferreira, F. Casse, Stationary Accretion Disks Launching Super-fast-magnetosonic Magnetohydrodynamic Jets. Astrophys. J. Lett. **601**, 139–142 (2004). doi:10.1086/381804

D.C. Gabuzda, VSOP observations of the compact BL Lacertae object 1803+784. New Astron. Rev. **43**, 691–694 (1999). doi:10.1016/S1387-6473(99)00079-2

D.C. Gabuzda, J.L. Gómez, VSOP polarization observations of the BL Lacertae object OJ 287. Mon. Not. Roy. Astron. Soc. **320**, 49–54 (2001). doi:10.1046/j.1365-8711.2001.04147.x

D.C. Gabuzda, É. Murray, P. Cronin, Helical magnetic fields associated with the relativistic jets of four BL Lac objects. Mon. Not. Roy. Astron. Soc. **351**, 89–93 (2004). doi:10.1111/j.1365-2966.2004.08037.x

D.C. Gabuzda, T.V. Cawthorne, D.H. Roberts, J.F.C. Wardle, A survey of the milliarcsecond polarization properties of BL Lacertae objects at 5 GHz. Astrophys. J. **388**, 40–54 (1992). doi:10.1086/171128

D.C. Gabuzda, C.M. Mullan, T.V. Cawthorne, J.F.C. Wardle, D.H. Roberts, Evolution of the milliarcsecond total intensity and polarization structures of BL Lacertae objects. Astrophys. J. **435**, 140–161 (1994). doi:10.1086/174801

D.C. Gabuzda, V.M. Vitrishchak, M. Mahmud, S.P. O'Sullivan, Radio circular polarization produced in helical magnetic fields in eight active galactic nuclei. Mon. Not. Roy. Astron. Soc. **384**, 1003–1014 (2008). doi:10.1111/j.1365-2966.2007.12773.x

D. Gabuzda, D. Christodoulou, I. Contopoulos, D. Kazanas, 2012 Evidence for Helical Magnetic fields in Kiloparsec-Scale AGN Jets and the Action of a Cosmic Battery. to be published in proceedings of the conference *Beamed and Unbeamed Gamma-rays from Radio Galaxies*, Muonio, Finland, 11-15 April 2011.

V. Gaibler, M. Krause, M. Camenzind, Very light magnetized jets on large scales - I. Evolution and magnetic fields. Mon. Not. Roy. Astron. Soc. **400**, 1785–1802 (2009). doi:10.1111/j.1365-2966.2009.15625.x

E. Gallo, R. Fender, C. Kaiser, D. Russell, R. Morganti, T. Oosterloo, S. Heinz, A dark jet dominates the power output of the stellar black hole Cygnus X-1. Nature **436**, 819–821 (2005). doi:10.1038/nature03879

J.L. Gómez, A.P. Marscher, S.G. Jorstad, I. Agudo, M. Roca-Sogorb, Faraday Rotation and Polarization Gradients in the Jet of 3C 120: Interaction with the External Medium and a Helical Magnetic Field? Astrophys. J. Lett. **681**, 69–72 (2008). doi:10.1086/590388

J. Gracia, N. Vlahakis, I. Agudo, K. Tsinganos, S.V. Bogovalov, Synthetic Synchrotron Emission Maps from MHD Models for the Jet of M87. Astrophys. J. **695**, 503–510 (2009). doi:10.1088/0004-637X/695/1/503

J. Granot, The Structure and Dynamics of GRB Jets, in *Revista Mexicana de Astronomia y Astrofisica, vol. 27*. Revista Mexicana de Astronomia y Astrofisica, vol. 27, vol. 27, 2007, pp. 140–165

R. Hallahan, D. Gabuzda, The Deca-parsec Scale Radio Structures of BL Lac Objects, in *The role of VLBI in the Golden Age for Radio Astronomy*, 2008

M.J. Hardcastle, Low-frequency constraints on the spectra of the lobes of the microquasar GRS 1758 258. Astron. Astrophys. **434**, 35–39 (2005). doi:10.1051/0004-6361:20041735

M.J. Hardcastle, Testing the beamed inverse-Compton model for jet X-ray emission: velocity structure and deceleration. Mon. Not. Roy. Astron. Soc. **366**, 1465–1474 (2006). doi:10.1111/j.1365-2966.2005.09923.x

M.J. Hardcastle, J.H. Croston, The Chandra view of extended X-ray emission from Pictor A. Mon. Not. Roy. Astron. Soc. **363**, 649–660 (2005). doi:10.1111/j.1365-2966.2005.09469.x

M.J. Hardcastle, J.H. Croston, Searching for the inverse-Compton emission from bright cluster-centre radio galaxies. Mon. Not. Roy. Astron. Soc. **404**, 2018–2027 (2010). doi:10.1111/j.1365-2966.2010.16420.x

M.J. Hardcastle, J.H. Croston, Modelling TeV γ-ray emission from the kiloparsec-scale jets of Centaurus A and M87. Mon. Not. Roy. Astron. Soc. **415**, 133–142 (2011). doi:10.1111/j.1365-2966.2011.18678.x

M.J. Hardcastle, L.W. Looney, The properties of powerful radio sources at 90 GHz. Mon. Not. Roy. Astron. Soc. **388**, 176–186 (2008). doi:10.1111/j.1365-2966.2008.13370.x

M.J. Hardcastle, M. Birkinshaw, D.M. Worrall, Magnetic field strengths in the hotspots of 3C 33 and 111. Mon. Not. Roy. Astron. Soc. **294**, 615 (1998). doi:10.1046/j.1365-8711.1998.01159.x

M.J. Hardcastle, M. Birkinshaw, D.M. Worrall, A Chandra detection of the radio hotspot of 3C123. Mon. Not. Roy. Astron. Soc. **323**, 17–22 (2001a). doi:10.1046/j.1365-8711.2001.04341.x

M.J. Hardcastle, M. Birkinshaw, D.M. Worrall, Chandra observations of the X-ray jet in 3C 66B. Mon. Not. Roy. Astron. Soc. **326**, 1499–1507 (2001b). doi:10.1046/j.1365-8711.2001.04699.x

M.J. Hardcastle, F. Massaro, D.E. Harris, X-ray emission from the extended emission-line region of the powerful radio galaxy 3C171. Mon. Not. Roy. Astron. Soc. **401**, 2697–2705 (2010). doi:10.1111/j.1365-2966.2009.15855.x

M.J. Hardcastle, P. Alexander, G.G. Pooley, J.M. Riley, High-resolution observations at 3.6cm of seventeen FRII radio galaxies with $0.15<z<0.30$. Mon. Not. Roy. Astron. Soc. **288**, 859–890 (1997)

M.J. Hardcastle, P. Alexander, G.G. Pooley, J.M. Riley, FR II radio galaxies with $z<0.3$ - II. Beaming and unification. Mon. Not. Roy. Astron. Soc. **304**, 135–144 (1999). doi:10.1046/j.1365-8711.1999.02298.x

M.J. Hardcastle, M. Birkinshaw, R.A. Cameron, D.E. Harris, L.W. Looney, D.M. Worrall, Magnetic Field Strengths in the Hot Spots and Lobes of Three Powerful Fanaroff-Riley Type II Radio Sources. Astrophys. J. **581**, 948–973 (2002). doi:10.1086/344409

M.J. Hardcastle, D.E. Harris, D.M. Worrall, M. Birkinshaw, The Origins of X-Ray Emission from the Hot Spots of FR II Radio Sources. Astrophys. J. **612**, 729–748 (2004). doi:10.1086/422808

M.J. Hardcastle, R.P. Kraft, G.R. Sivakoff, J.L. Goodger, J.H. Croston, A. Jordán, D.A. Evans, D.M. Worrall, M. Birkinshaw, S. Raychaudhury, N.J. Brassington, W.R. Forman, W.E. Harris, C. Jones, A.M. Juett, S.S. Murray, P.E.J. Nulsen, C.L. Sarazin, K.A. Woodley, New Results on Particle Acceleration in the Centaurus A Jet and Counterjet from a Deep Chandra Observation. Astrophys. J. Lett. **670**, 81–84 (2007). doi:10.1086/524197

P.E. Hardee, A. Rosen, On the Dynamics and Structure of Three-dimensional Trans-Alfvénic Jets. Astrophys. J. **524**, 650–666 (1999). doi:10.1086/307833

D.E. Harris, J.E. Grindlay, The prospects for X-ray detection of inverse-Compton emission from radio source electrons and photons of the microwave background. Mon. Not. Roy. Astron. Soc. **188**, 25–37 (1979)

D.E. Harris, H. Krawczynski, X-Ray Emission from Extragalactic Jets. Ann. Rev. Astron. Astrophys. **44**, 463–506 (2006). doi:10.1146/annurev.astro.44.051905.092446

D.E. Harris, C.L. Carilli, R.A. Perley, X-ray emission from the radio hotspots of Cygnus A. Nature **367**, 713–716 (1994). doi:10.1038/367713a0

D.E. Harris, K.M. Leighly, J.P. Leahy, X-Ray Emission from a Radio Hot Spot in 3C 390.3: Evidence for the Deflection of a Radio Jet by a Neighboring Galaxy. Astrophys. J. Lett. **499**, 149 (1998). doi:10.1086/311365

D.E. Harris, P.E.J. Nulsen, T.J. Ponman, M. Bautz, R.A. Cameron, L.P. David, R.H. Donnelly, W.R. Forman, L. Grego, M.J. Hardcastle, J.P. Henry, C. Jones, J.P. Leahy, M. Markevitch, A.R. Martel, B.R. McNamara, P. Mazzotta, W. Tucker, S.N. Virani, J. Vrtilek, Chandra X-Ray Detection of the Radio Hot Spots of 3C 295. Astrophys. J. Lett. **530**, 81–84 (2000). doi:10.1086/312503

S. Heinz, Radio lobe dynamics and the environment of microquasars. Astron. Astrophys. **388**, 40–43 (2002). doi:10.1051/0004-6361:20020402

P. Hennebelle, S. Fromang, Magnetic processes in a collapsing dense core. I. Accretion and ejection. Astron. Astrophys. **477**, 9–24 (2008). doi:10.1051/0004-6361:20078309

J. Heyvaerts, C. Norman, The collimation of magnetized winds. Astrophys. J. **347**, 1055–1081 (1989). doi:10.1086/168195

T. Hovatta, M. Lister, M. Aller, H. Aller, D. Homan, Y. Kovalev, A. Pushkarev, 2012 MOJAVE: Monitoring of Jets in Active Galactic Nuclei with VLBA Experiments. VIII. Faraday rotation in parsec-scale AGN jets. Submitted to AJ

M. Huarte-Espinosa, M. Krause, P. Alexander, 3D magnetohydrodynamic simulations of the evolution of magnetic fields in Fanaroff-Riley class II radio sources. Mon. Not. Roy. Astron. Soc. **417**, 382–399 (2011). doi:10.1111/j.1365-2966.2011.19271.x

P.A. Hughes, H.D. Aller, M.F. Aller, Synchrotron Emission from Shocked Relativistic Jets. II. A Model for the Centimeter Wave Band Quiescent and Burst Emission from BL Lacertae. Astrophys. J. **341**, 68 (1989). doi:10.1086/167472

N. Isobe, M. Tashiro, K. Makishima, N. Iyomoto, M. Suzuki, M.M. Murakami, M. Mori, K. Abe, A Chandra Detection of Diffuse Hard X-Ray Emission Associated with the Lobes of the Radio Galaxy 3C 452. Astrophys. J. Lett. **580**, 111–115 (2002). doi:10.1086/345658

S. Jester, H.J. Röser, K. Meisenheimer, R. Perley, X-rays from the jet in 3C 273: Clues from the radio-optical spectra. Astron. Astrophys. **385**, 27–30 (2002). doi:10.1051/0004-6361:20020278

S. Jester, H.J. Röser, K. Meisenheimer, R. Perley, The radio-ultraviolet spectral energy distribution of the jet in 3C 273. Astron. Astrophys. **431**, 477–502 (2005). doi:10.1051/0004-6361:20047021

N.N. Jetha, M.J. Hardcastle, A. Babul, E. O'Sullivan, T.J. Ponman, S. Raychaudhury, J. Vrtilek, The nature of the ghost cavity in the NGC 741 group. Mon. Not. Roy. Astron. Soc. **384**, 1344–1354 (2008). doi:10.1111/j.1365-2966.2007.12829.x

C.M. Johns-Krull, The Magnetic Fields of Classical T Tauri Stars. Astrophys. J. **664**, 975–985 (2007). doi:10.1086/519017

T.W. Jones, D. Ryu, A. Engel, Simulating Electron Transport and Synchrotron Emission in Radio Galaxies: Shock Acceleration and Synchrotron Aging in Axisymmetric Flows. Astrophys. J. **512**, 105–124 (1999). doi:10.1086/306772

C.R. Kaiser, P. Alexander, A self-similar model for extragalactic radio sources. Mon. Not. Roy. Astron. Soc. **286**, 215–222 (1997)

J. Kataoka, Ł. Stawarz, X-Ray Emission Properties of Large-Scale Jets, Hot Spots, and Lobes in Active Galactic Nuclei. Astrophys. J. **622**, 797–810 (2005). doi:10.1086/428083

P. Kharb, D.C. Gabuzda, C.P. O'Dea, P. Shastri, S.A. Baum, Rotation Measures Across Parsec-Scale Jets of Fanaroff-Riley Type I Radio Galaxies. Astrophys. J. **694**, 1485–1497 (2009). doi:10.1088/0004-637X/694/2/1485

A. Konigl, Relativistic jets as X-ray and gamma-ray sources. Astrophys. J. **243**, 700–709 (1981). doi:10.1086/158638

A. Königl, Disk accretion onto magnetic T Tauri stars. Astrophys. J. Lett. **370**, 39–43 (1991).

doi:10.1086/185972
R. Krasnopolsky, Z.Y. Li, R. Blandford, Magnetocentrifugal Launching of Jets from Accretion Disks. I. Cold Axisymmetric Flows. Astrophys. J. **526**, 631–642 (1999). doi:10.1086/308023
M. Krause, Very light jets II: Bipolar large scale simulations in King atmospheres. Astron. Astrophys. **431**, 45–64 (2005). doi:10.1051/0004-6361:20041191
P.P. Kronberg, R.V.E. Lovelace, G. Lapenta, S.A. Colgate, Measurement of the Electric Current in a kpc-scale Jet. Astrophys. J. Lett. **741**, 15 (2011). doi:10.1088/2041-8205/741/1/L15
T. Kudoh, R. Matsumoto, K. Shibata, Are Jets Ejected from Locally Magnetized Accretion Disks? Proc. Astron. Soc. Jpn. **54**, 267–274 (2002)
R.A. Laing, A model for the magnetic-field structure in extended radio sources. Mon. Not. Roy. Astron. Soc. **193**, 439–449 (1980)
R.A. Laing, Interpretation of Radio Polarization Data, in *Physics of Energy Transport in Extragalactic Radio Sources*, ed. by A. H. Bridle, 1984, p. 90
R.A. Laing, A.H. Bridle, Relativistic models and the jet velocity field in the radio galaxy 3C 31. Mon. Not. Roy. Astron. Soc. **336**, 328–352 (2002). doi:10.1046/j.1365-8711.2002.05756.x
R.A. Laing, J.R. Canvin, A.H. Bridle, M.J. Hardcastle, A relativistic model of the radio jets in 3C296. Mon. Not. Roy. Astron. Soc. **372**, 510–536 (2006). doi:10.1111/j.1365-2966.2006.10903.x
R.A. Laing, A.H. Bridle, P. Parma, M. Murgia, Structures of the magnetoionic media around the Fanaroff-Riley Class I radio galaxies 3C31 and Hydra A. Mon. Not. Roy. Astron. Soc. **391**, 521–549 (2008). doi:10.1111/j.1365-2966.2008.13895.x
J.P. Leahy, A.R.S. Black, J. Dennett-Thorpe, M.J. Hardcastle, S. Komissarov, R.A. Perley, J.M. Riley, P.A.G. Scheuer, A study of FRII radio galaxies with z$<$0.15 - II. High-resolution maps of 11 sources at 3.6 CM. Mon. Not. Roy. Astron. Soc. **291**, 20–53 (1997)
C.F. Lee, L.G. Mundy, B. Reipurth, E.C. Ostriker, J.M. Stone, CO Outflows from Young Stars: Confronting the Jet and Wind Models. Astrophys. J. **542**, 925–945 (2000). doi:10.1086/317056
P. Lii, M. Romanova, R. Lovelace, Magnetic launching and collimation of jets from the disc-magnetosphere boundary: 2.5D MHD simulations. Mon. Not. Roy. Astron. Soc. **420**, 2020–2033 (2012). doi:10.1111/j.1365-2966.2011.20133.x
M.L. Lister, D.C. Homan, MOJAVE: Monitoring of Jets in Active Galactic Nuclei with VLBA Experiments. I. First-Epoch 15 GHz Linear Polarization Images. Astron. J. **130**, 1389–1417 (2005). doi:10.1086/432969
A.P. Lobanov, Ultracompact jets in active galactic nuclei. Astron. Astrophys. **330**, 79–89 (1998)
D. Lynden-Bell, Magnetic collimation by accretion discs of quasars and stars. Mon. Not. Roy. Astron. Soc. **279**, 389–401 (1996)
D. Lynden-Bell, On why discs generate magnetic towers and collimate jets. Mon. Not. Roy. Astron. Soc. **341**, 1360–1372 (2003). doi:10.1046/j.1365-8711.2003.06506.x
M. Lyutikov, V.I. Pariev, D.C. Gabuzda, Polarization and structure of relativistic parsec-scale AGN jets. Mon. Not. Roy. Astron. Soc. **360**, 869–891 (2005). doi:10.1111/j.1365-2966.2005.08954.x
M. Mahmud, Searching for Helical Magnetic Fields in Active Galactic Nuclei, PhD thesis, University College Cork, 2010
M. Mahmud, D. Gabuzda, Using Faraday Rotation Gradients to probe Magnetic Tower Models, in *The role of VLBI in the Golden Age for Radio Astronomy*, 2008
M. Mahmud, D.C. Gabuzda, V. Bezrukovs, Surprising evolution of the parsec-scale Faraday Rotation gradients in the jet of the BL Lac object B1803+784. Mon. Not. Roy. Astron. Soc. **400**, 2–12 (2009). doi:10.1111/j.1365-2966.2009.15013.x
M. Mahmud, D. Gabuzda, C. Coughlan, D. Hallahan, 2012 Connecting Magnetic Towers with Faraday Rotation Gradients in Active Galactic Nuclei Jets. Submitted to MNRAS.
H.L. Marshall, M.J. Hardcastle, M. Birkinshaw, J. Croston, D. Evans, H. Landt, E. Lenc, F. Massaro, E.S. Perlman, D.A. Schwartz, A. Siemiginowska, Ł. Stawarz, C.M. Urry, D.M. Worrall, A Flare in the Jet of Pictor A. Astrophys. J. Lett. **714**, 213–216 (2010). doi:10.1088/2041-8205/714/2/L213
S. Matt, R.E. Pudritz, Does Disk Locking Solve the Stellar Angular Momentum Problem? Astrophys. J. Lett. **607**, 43–46 (2004). doi:10.1086/421351
S. Matt, R.E. Pudritz, Accretion-powered Stellar Winds as a Solution to the Stellar Angular Momentum Problem. Astrophys. J. Lett. **632**, 135–138 (2005). doi:10.1086/498066
S. Matt, R.E. Pudritz, Accretion-powered Stellar Winds. II. Numerical Solutions for Stellar Wind Torques. Astrophys. J. **678**, 1109–1118 (2008). doi:10.1086/533428
A.P. Matthews, P.A.G. Scheuer, Models of Radio Galaxies with Tangled Magnetic Fields - Part Two - Numerical Simulations and Their Interpretation. Mon. Not. Roy. Astron. Soc. **242**, 623 (1990)
J.C. McKinney, General relativistic magnetohydrodynamic simulations of the jet formation and large-scale propagation from black hole accretion systems. Mon. Not. Roy. Astron. Soc. **368**, 1561–1582 (2006). doi:10.1111/j.1365-2966.2006.10256.x

J.C. McKinney, R.D. Blandford, Stability of relativistic jets from rotating, accreting black holes via fully three-dimensional magnetohydrodynamic simulations. Mon. Not. Roy. Astron. Soc. **394**, 126–130 (2009). doi:10.1111/j.1745-3933.2009.00625.x

J.C. McKinney, A. Tchekhovskoy, R.D. Blandford, General Relativistic Magnetohydrodynamic Simulations of Magnetically Choked Accretion Flows around Black Holes. Mon. Not. Roy. Astron. Soc. **in press**, (2012)

R.R. Mellon, Z.Y. Li, Magnetic Braking and Protostellar Disk Formation: The Ideal MHD Limit. Astrophys. J. **681**, 1356–1376 (2008). doi:10.1086/587542

P. Mendygral, T. Jones, K. Dolag, MHD Simulations of AGN Jets in a Dynamic Galaxy Cluster Medium. Astrophys. J. **in press**, (2012)

L. Mestel, Magnetic braking by a stellar wind-I. Mon. Not. Roy. Astron. Soc. **138**, 359 (1968)

P. Mészáros, Gamma Ray Bursts. Astropart. Phys **in press**, (2012)

F.C. Michel, Relativistic Stellar-Wind Torques. Astrophys. J. **158**, 727 (1969). doi:10.1086/150233

A. Mignone, P. Rossi, G. Bodo, A. Ferrari, S. Massaglia, High-resolution 3D relativistic MHD simulations of jets. Mon. Not. Roy. Astron. Soc. **402**, 7–12 (2010). doi:10.1111/j.1365-2966.2009.15642.x

P. Mimica, M.A. Aloy, I. Agudo, J.M. Martí, J.L. Gómez, J.A. Miralles, Spectral Evolution of Superluminal Components in Parsec-Scale Jets. Astrophys. J. **696**, 1142–1163 (2009). doi:10.1088/0004-637X/696/2/1142

I.F. Mirabel, Black Hole Jet Sources, in *The Tenth Marcel Grossmann Meeting. On recent developments in theoretical and experimental general relativity, gravitation and relativistic field theories*, ed. by M. Novello, S. Perez Bergliaffa, & R. Ruffini, 2005, p. 606. doi:10.1142/9789812704030_0037

I.F. Mirabel, L.F. Rodriguez, B. Cordier, J. Paul, F. Lebrun, A double-sided radio jet from the compact Galactic Centre annihilator 1E140.7 - 2942. Nature **358**, 215–217 (1992). doi:10.1038/358215a0

T.C. Mouschovias, Nonhomologous contraction and equilibria of self-gravitating, magnetic interstellar clouds embedded in an intercloud medium: Star formation. I Formulation of the problem and method of solution. Astrophys. J. **206**, 753–767 (1976). doi:10.1086/154436

L.M. Mullin, M.J. Hardcastle, Bayesian inference of jet bulk-flow speeds in Fanaroff-Riley type II radio sources. Mon. Not. Roy. Astron. Soc. **398**, 1989–2004 (2009). doi:10.1111/j.1365-2966.2009.15232.x

L.M. Mullin, J.M. Riley, M.J. Hardcastle, Observed properties of FRII quasars and radio galaxies at $z < 1.0$. Mon. Not. Roy. Astron. Soc. **390**, 595–621 (2008). doi:10.1111/j.1365-2966.2008.13534.x

E. Murphy, D.C. Gabuzda, Investigating the Effects of Finite Resolution on Observed Transverse Jet Profiles. Journal of Physics Conference Series **355**(1), 012009 (2012). doi:10.1088/1742-6596/355/1/012009

E. Murphy, D. Gabuzda, T. Cawthorne, Gleaning secrets from the transverse proles of AGN jets, in *"Proceedings of the 10th European VLBI Network Symposium and EVN Users Meeting: VLBI and the new generation of radio arrays. September 20-24, 2010. Manchester, UK. Published online at http://pos.sissa.it/cgi-bin/reader/conf.cgi?confid=125, id.41"*, 2010

E. Murphy, D. Gabuzda, T. Cawthorne, 2012 Analysing the Transverse Structure of the Relativistic Jets of AGN. Submitted to MNRAS.

S.T. Myers, S.R. Spangler, Synchrotron aging in the lobes of luminous radio galaxies. Astrophys. J. **291**, 52–62 (1985). doi:10.1086/163040

M. Nakamura, H. Li, S. Li, Structure of Magnetic Tower Jets in Stratified Atmospheres. Astrophys. J. **652**, 1059–1067 (2006). doi:10.1086/508338

S.M. O'Neill, T.W. Jones, Three-Dimensional Simulations of Bi-Directed Magnetohydrodynamic Jets Interacting with Cluster Environments. Astrophys. J. **710**, 180–196 (2010). doi:10.1088/0004-637X/710/1/180

S.M. O'Neill, I.L. Tregillis, T.W. Jones, D. Ryu, Three-dimensional Simulations of MHD Jet Propagation through Uniform and Stratified External Environments. Astrophys. J. **633**, 717–732 (2005). doi:10.1086/491618

S.P. O'Sullivan, D.C. Gabuzda, Magnetic field strength and spectral distribution of six parsec-scale active galactic nuclei jets. Mon. Not. Roy. Astron. Soc. **400**, 26–42 (2009a). doi:10.1111/j.1365-2966.2009.15428.x

S.P. O'Sullivan, D.C. Gabuzda, Three-dimensional magnetic field structure of six parsec-scale active galactic nuclei jets. Mon. Not. Roy. Astron. Soc. **393**, 429–456 (2009b). doi:10.1111/j.1365-2966.2008.14213.x

R. Ouyed, R.E. Pudritz, Numerical Simulations of Astrophysical Jets from Keplerian Disks. I. Stationary Models. Astrophys. J. **482**, 712 (1997). doi:10.1086/304170

R. Ouyed, D.A. Clarke, R.E. Pudritz, Three-dimensional Simulations of Jets from Keplerian Disks: Self-regulatory Stability. Astrophys. J. **582**, 292–319 (2003). doi:10.1086/344507

R. Ouyed, R.E. Pudritz, J.M. Stone, Episodic jets from black holes and protostars. Nature **385**, 409–414 (1997). doi:10.1038/385409a0

G. Pelletier, R.E. Pudritz, Hydromagnetic disk winds in young stellar objects and active galactic nuclei.

Astrophys. J. **394**, 117–138 (1992). doi:10.1086/171565
R.A. Perley, C.L. Carilli, The structure and polarization of Cygnus A at λ 3.6cm, ed. by Carilli, C. L. & Harris, D. E. 1996, p. 168
R.A. Perley, H.J. Roser, K. Meisenheimer, The radio galaxy PictorA – a study with the VLA. Astron. Astrophys. **328**, 12–32 (1997)
T. Piran, The physics of gamma-ray bursts. Reviews of Modern Physics **76**, 1143–1210 (2004). doi:10.1103/RevModPhys.76.1143
O. Porth, C. Fendt, Acceleration and Collimation of Relativistic Magnetohydrodynamic Disk Winds. Astrophys. J. **709**, 1100–1118 (2010). doi:10.1088/0004-637X/709/2/1100
O. Porth, C. Fendt, Z. Meliani, B. Vaidya, Synchrotron Radiation of Self-collimating Relativistic Magnetohydrodynamic Jets. Astrophys. J. **737**, 42 (2011). doi:10.1088/0004-637X/737/1/42
R.E. Pudritz, C.A. Norman, Centrifugally driven winds from contracting molecular disks. Astrophys. J. **274**, 677–697 (1983). doi:10.1086/161481
R.E. Pudritz, C.A. Norman, Bipolar hydromagnetic winds from disks around protostellar objects. Astrophys. J. **301**, 571–586 (1986). doi:10.1086/163924
R.E. Pudritz, C.S. Rogers, R. Ouyed, Controlling the collimation and rotation of hydromagnetic disc winds. Mon. Not. Roy. Astron. Soc. **365**, 1131–1148 (2006). doi:10.1111/j.1365-2966.2005.09766.x
R.E. Pudritz, R. Ouyed, C. Fendt, A. Brandenburg, Disk Winds, Jets, and Outflows: Theoretical and Computational Foundations, in *Protostars and Planets V*, ed. by B. Reipurth, D. Jewitt, K. Keil, 2007, pp. 277–294
A.B. Pushkarev, D.C. Gabuzda, Y.N. Vetukhnovskaya, V.E. Yakimov, Spine-sheath polarization structures in four active galactic nuclei jets. Mon. Not. Roy. Astron. Soc. **356**, 859–871 (2005). doi:10.1111/j.1365-2966.2004.08535.x
T.P. Ray, Kelvin-Helmholtz instabilities in radio jets. Mon. Not. Roy. Astron. Soc. **196**, 195–207 (1981)
T. Ray, C. Dougados, F. Bacciotti, J. Eislöffel, A. Chrysostomou, Toward Resolving the Outflow Engine: An Observational Perspective, in *Protostars and Planets V*, ed. by B. Reipurth, D. Jewitt, K. Keil, 2007, pp. 231–244
A. Reichstein, D. Gabuzda, Studying magnetic fields in several parsec-scale AGN jets using Faraday rotation, in *"Proceedings of the 10th European VLBI Network Symposium and EVN Users Meeting: VLBI and the new generation of radio arrays. September 20-24, 2010. Manchester, UK. Published online at http://pos.sissa.it/cgi-bin/reader/conf.cgi?confid=125, id.44"*, 2010
M.M. Romanova, G.V. Ustyugova, A.V. Koldoba, V.M. Chechetkin, R.V.E. Lovelace, Formation of Stationary Magnetohydrodynamic Outflows from a Disk by Time-dependent Simulations. Astrophys. J. **482**, 708 (1997). doi:10.1086/304199
M.M. Romanova, G.V. Ustyugova, A.V. Koldoba, R.V.E. Lovelace, Magnetohydrodynamic Simulations of Disk-Magnetized Star Interactions in the Quiescent Regime: Funnel Flows and Angular Momentum Transport. Astrophys. J. **578**, 420–438 (2002). doi:10.1086/342464
M.M. Romanova, G.V. Ustyugova, A.V. Koldoba, R.V.E. Lovelace, MRI-driven accretion on to magnetized stars: global 3D MHD simulations of magnetospheric and boundary layer regimes. Mon. Not. Roy. Astron. Soc. **421**, 63–77 (2012). doi:10.1111/j.1365-2966.2011.20055.x
P.A.G. Scheuer, Models of extragalactic radio sources with a continuous energy supply from a central object. Mon. Not. Roy. Astron. Soc. **166**, 513–528 (1974)
D.A. Schwartz, H.L. Marshall, J.E.J. Lovell, B.G. Piner, S.J. Tingay, M. Birkinshaw, G. Chartas, M. Elvis, E.D. Feigelson, K.K. Ghosh, D.E. Harris, H. Hirabayashi, E.J. Hooper, D.L. Jauncey, K.M. Lanzetta, S. Mathur, R.A. Preston, W.H. Tucker, S. Virani, B. Wilkes, D.M. Worrall, Chandra Discovery of a 100 kiloparsec X-Ray Jet in PKS 0637-752. Astrophys. J. Lett. **540**, 69 (2000). doi:10.1086/312875
D. Seifried, R. Banerjee, R.S. Klessen, D. Duffin, R.E. Pudritz, Magnetic fields during the early stages of massive star formation - I. Accretion and disc evolution. Mon. Not. Roy. Astron. Soc. **417**, 1054–1073 (2011). doi:10.1111/j.1365-2966.2011.19320.x
D. Seifried, R.E. Pudritz, R. Banerjee, D. Duffin, R.S. Klessen, Magnetic fields during the early stages of massive star formation - II. A generalised outflow criterion. Mon. Not. Roy. Astron. Soc. **in press**, (2012)
F.H. Shu, J.R. Najita, H. Shang, Z.Y. Li, X-Winds Theory and Observations, in *Protostars and Planets IV*, ed. by V. Mannings, A. Boss, S. Russell, 2000, p. 789
R. Soria, M.W. Pakull, J.W. Broderick, S. Corbel, C. Motch, Radio lobes and X-ray hotspots in the microquasar S26. Mon. Not. Roy. Astron. Soc. **409**, 541–551 (2010). doi:10.1111/j.1365-2966.2010.17360.x
H.C. Spruit, Theory of Magnetically Powered Jets, in *Lecture Notes in Physics, Berlin Springer Verlag*, ed. by T. Belloni. Lecture Notes in Physics, Berlin Springer Verlag, vol. 794, 2010, p. 233. doi:10.1007/978-3-540-76937-8_9
J.E. Staff, B.P. Niebergal, R. Ouyed, R.E. Pudritz, K. Cai, Confronting Three-dimensional Time-dependent

Jet Simulations with Hubble Space Telescope Observations. Astrophys. J. **722**, 1325–1332 (2010). doi:10.1088/0004-637X/722/2/1325

Ł. Stawarz, M. Sikora, M. Ostrowski, High-Energy Gamma Rays from FR I Jets. Astrophys. J. **597**, 186–201 (2003). doi:10.1086/378290

F. Tavecchio, L. Maraschi, R.M. Sambruna, C.M. Urry, The X-Ray Jet of PKS 0637-752: Inverse Compton Radiation from the Cosmic Microwave Background? Astrophys. J. Lett. **544**, 23–26 (2000). doi:10.1086/317292

G.B. Taylor, R. Zavala, Are There Rotation Measure Gradients Across Active Galactic Nuclei Jets? Astrophys. J. Lett. **722**, 183–187 (2010). doi:10.1088/2041-8205/722/2/L183

I.L. Tregillis, T.W. Jones, D. Ryu, Simulating Electron Transport and Synchrotron Emission in Radio Galaxies: Shock Acceleration and Synchrotron Aging in Three-dimensional Flows. Astrophys. J. **557**, 475–491 (2001). doi:10.1086/321657

I.L. Tregillis, T.W. Jones, D. Ryu, Synthetic Observations of Simulated Radio Galaxies. I. Radio and X-Ray Analysis. Astrophys. J. **601**, 778–797 (2004). doi:10.1086/380756

T. Velusamy, W.D. Langer, K.A. Marsh, Highly Collimated Jets and Wide-Angle Outflows in HH 46/47: New Evidence from Spitzer Infrared Images. Astrophys. J. Lett. **668**, 159–162 (2007). doi:10.1086/522929

T. Velusamy, W.D. Langer, M.S.N. Kumar, J.M.C. Grave, Jets and Wide-angle Outflows in Cepheus E: New Evidence from Spitzer. Astrophys. J. **741**, 60 (2011). doi:10.1088/0004-637X/741/1/60

N. Vlahakis, A. Königl, Relativistic Magnetohydrodynamics with Application to Gamma-Ray Burst Outflows. I. Theory and Semianalytic Trans-Alfvénic Solutions. Astrophys. J. **596**, 1080–1103 (2003). doi:10.1086/378226

B. von Rekowski, A. Brandenburg, Structured, Dynamo Driven Stellar and Disc Winds, in *Asymmetrical Planetary Nebulae III: Winds, Structure and the Thunderbird*, ed. by M. Meixner, J. H. Kastner, B. Balick, & N. Soker. Astronomical Society of the Pacific Conference Series, vol. 313, 2004, p. 476

J.F.C. Wardle, S.E. Aaron, How fast are the large-scale jets in quasars? Constraints on both Doppler beaming and intrinsic asymmetries. Mon. Not. Roy. Astron. Soc. **286**, 425–435 (1997)

E.T. Whelan, T.P. Ray, L. Podio, F. Bacciotti, S. Randich, Classical T Tauri-like Outflow Activity in the Brown Dwarf Mass Regime. Astrophys. J. **706**, 1054–1068 (2009). doi:10.1088/0004-637X/706/2/1054

A.S. Wilson, D.A. Smith, A.J. Young, The Cavity of Cygnus A. Astrophys. J. Lett. **644**, 9–12 (2006). doi:10.1086/504108

A.S. Wilson, A.J. Young, P.L. Shopbell, Chandra X-Ray Observations of Pictor A: High-Energy Cosmic Rays in a Radio Galaxy. Astrophys. J. **547**, 740–753 (2001). doi:10.1086/318412

N.L. Zakamska, M.C. Begelman, R.D. Blandford, Hot Self-similar Relativistic Magnetohydrodynamic Flows. Astrophys. J. **679**, 990–999 (2008). doi:10.1086/587870

C. Zanni, A. Ferrari, R. Rosner, G. Bodo, S. Massaglia, MHD simulations of jet acceleration from Keplerian accretion disks. The effects of disk resistivity. Astron. Astrophys. **469**, 811–828 (2007). doi:10.1051/0004-6361:20066400

R.T. Zavala, G.B. Taylor, A View through Faraday's Fog: Parsec-Scale Rotation Measures in Active Galactic Nuclei. Astrophys. J. **589**, 126–146 (2003). doi:10.1086/374619

R.T. Zavala, G.B. Taylor, A View through Faraday's Fog. II. Parsec-Scale Rotation Measures in 40 Active Galactic Nuclei. Astrophys. J. **612**, 749–779 (2004). doi:10.1086/422741

R.T. Zavala, G.B. Taylor, Faraday Rotation Measure Gradients from a Helical Magnetic Field in 3C 273. Astrophys. J. Lett. **626**, 73–76 (2005). doi:10.1086/431901